

Supplemental Material

Supplemental Methods

Genotyping *Kihl40* and MCK-*Kihl40* mice. *Kihl40* genotypes were determined based on the presence or absence of the targeted allele and the presence or absence of the wild type (WT) allele using two separate genotyping reactions. The genotyping primer set used to determine the presence of the targeted allele was (amplifies *LacZ* sequence): F – ttatcgatgagcgtgggtggtatgc, R – gcgctacatcgggcaaataatc. The genotyping primer set used to determine the presence of the WT allele was: F – aggggtgggggcagagaca, R – agctgccctctcctcctcc.

Presence of the *MCK-Kihl40* transgene was determined by genotyping using qPCR primers for *Kihl40* expression analysis (see below).

Echocardiography studies. Echocardiography was performed on P5 neonates using the Vevo 2100 small animal echocardiography system (VisualSonics) and a 40-MHz transducer. Pups were kept on a heating pad before and after the procedure to avoid a vagal response. Conscious pups were gently restrained and the ultrasound probe positioned to obtain a parasternal short-axis view. The largest anteroposterior diameters in diastole and systole were assessed in at least three recorded M-mode tracings and LV fractional shortening calculated according to the formula $FS(\%) = [(LVIDd - LVIDs)/LVIDd] \times 100$. Heart rate was assessed to exclude a vagal response. Data were analyzed by a single observer.

Radioactive in situ hybridization. Radioisotopic *in situ* hybridization on embryonic section was performed as previously described (1). The probe used to track *Klhl40* expression contained the full-length *Klhl40* coding sequence.

Northern blot analysis. A pre-made adult mouse multi-tissue Northern blot was purchased from Zyagen (MN-MT-1) and then was analyzed as previously described (2). *Klhl40* probe was generated by labelling a 802nt fragment that spanned nt 400-1201 of *Klhl40* cDNA (NCBI reference sequence NM_028202.3) with [α -³²P]dCTP using the RadPrime DNA Labelling System (Invitrogen). For *Gapdh* loading control, the blot was used without stripping and incubated with *Gapdh* probe generated from full-length *Gapdh* coding sequence using the all the same steps as mentioned above.

Quantitative real-time PCR (qPCR). Total RNA was extracted from either mouse tissue or cultured cells with TRIZOL (Invitrogen) according to manufacturer instructions. cDNA was synthesized using Superscript III reverse transcriptase with random hexamer primers (Invitrogen). Gene expression was analyzed by qPCR using either Power SYBR Green or Taqman Master Mix (Life Technologies) or KAPA SYBR FAST (Kapa Biosystems). The following primers (in order of appearance) were used for SYBR analysis: *Klhl40* – F: cccaagaacctgtcagctctggtgac, R: tcagagtccaagtggtcaaaactgcag; *Lmod2* – F: ttggagaaggaacggctggg R: cctcagagacttcgctgttgctctc, *Lmod3* (used to analyzed *Lmod3-myc* as well) – F: ccgctggtggaaatcactccc, R: actccagctccttggcagttgc; *Neb_{frag}-myc* F: ggttgctatgcctatgatacccctg, R: tgcctgttaattggacagtcagcaac. *Neb* was analyzed using a Taqman probe (ID: Mm01546298_1) purchased from Life

Technologies. All analyses were performed on a 7900HT Fast Real-Time PCR machine (Life Technologies).

Thin filament length analysis by actin immunofluorescence. P5 K1h140 WT and KO tibialis anterior muscles (TA) were prepared for thin filament analysis as previously described (3).

TA sections were incubated at 55°C for 10 minutes followed by blocking for 30 minutes in PBS/1% BSA, 1% heat inactivated goat serum, 0.025% Tween-20. Next, sections were incubated with a 1:400 dilution of Alexa Fluor 594 phalloidin (Life Technologies) for 1 hour to label actin. Sections were washed, mounted, and imaged as described in the previous section.

To estimate thin filament lengths, we performed line scan analysis on selected thin filament arrays of 3-6 sarcomeres that ran perpendicularly to the length of the myofibril. In total, we selected three arrays each from a total of two K1h140 WT and KO muscles, and calculated the lengths of 32 and 26 sarcomeres from WT and KO muscles, respectively. We estimated thin-filament length as done in previous studies, but at 1/10th maximal intensity for each peak (4). All analyses of thin filament arrays were done using Fiji ImageJ software (5).

X-gal staining of whole tissue or muscle sections. X-gal staining was done as previously described (2).

Cloning of epitope tagged constructs for electroporation, protein stability, and immunoprecipitation experiments. The *Klhl40*, *Actn1a*, *Tmod4*, and *Lmod3* coding sequence was subcloned into pcDNA3-EGFP to create C-terminally fused EGFP constructs (respectively referred to as Klhl40-EGFP, Actn1a-EGFP, Tmod4-EGFP, and Lmod3-EGFP) for electroporation.

In addition, the *Klhl40* CDS was subcloned into a p3XFLAG-CMV-10 vector modified with a tandem HA tag (p3XFLAG-CMV-10-NHA) and also subcloned into a custom pcDNA3.1-Hygro vector with a HA-3XFLAG (pcDNA3.1/Hygro(+)-C-HA-3XFLAG) tandem tag for N-terminal 3XFLAG-HA and C-terminal HA-3XFLAG fusion, respectively. N-terminal fused Klhl40 is referred to as 3XFLAG-HA-Klhl40 or FLAG-Klhl40 while C-terminally fused Klhl40 is referred to as Klhl40-HA-3XFLAG. Both N- and C-terminally fused Klhl40 constructs were subcloned into the pBabe-X retroviral vector (referred to as pBX-3XFLAG-HA-Klhl40 and pBX-Klhl40-3XFLAG-HA, respectively) (6). Full length EGFP was also N-terminally fused with 3XFLAG-HA (3XFLAG-HA-EGFP) and subcloned into pBabe-X (pBX-3XFLAG-HA-EGFP).

Neb_{frag}-myc was generated by cloning the cDNA sequence corresponding to the protein fragment of Neb identified from the Klhl40 yeast two-hybrid analysis (NCBI reference sequence NM_010889.1, nucleotides 17627-18221) with an added Kozak sequence and a translational start site (CGC CAC CAT G). Neb_{frag} and full length Lmod3 was C-terminally myc tagged by cloning into pcDNA3.1(+)/myc-His A (Invitrogen).

C2C12 infection, protein extraction and mass spectrometry for tandem affinity purification (TAP). 26µg of the pBX-3XFLAG-HA-EGFP, pBX-3XFLAG-HA-KIhl40, and pBX-KIhl40-HA-3XFLAG retroviral constructs were transfected into 80% confluent Platinum E cells (Cell Biolabs) on 15cm plates using Fugene 6 (Promega) at a 3:1 DNA to Fugene 6 ratio according to manufacturer's directions. Viral media was collected at 24 and 48 hours post-transfection by drawing off media and filtering through a 0.45µm syringe filter (Corning). Polybrene was added to viral media to a final concentration of 10µg/mL. Following filtration, viral media was added immediately to 100% confluent C2C12 myoblasts (from American Type Culture Collection) in growth media (DMEM with 10% fetal bovine serum [FBS; Life Technologies] and 1% antibiotic-antimycotic [Life Technologies]) on 15cm plates coated with 0.1% agar at 24 and 48 hours after transfection. After allowing the second infection to occur overnight, C2C12 cells were washed with PBS and then differentiated for 5 days with differentiation media (DMEM with 2% horse serum [HS; Life Technologies] and 1% antibiotic-antimycotic).

Protein was collected from C2C12 myotubes by washing cells and then collecting them into 5mL PBS by scraping cells with a sterile cell lifter. Protein extraction and FLAG-HA tandem affinity purification was done as previously described except with 2.4mg of starting protein material (7).

Tandem affinity purified protein samples were loaded into an Any kD Mini-PROTEAN TGX Gel (Bio-Rad) and ran according to standard SDS-PAGE procedures followed by silver staining, cutting of protein bands, and peptide extraction for mass spectrometry as previously described (7).

The extracted peptides were separated using an analytical capillary column (100 μ m x 12cm) packed with 3 μ m of spherical C18 reversed phase material with 100Å pore size and 2.7 μ m particle size (Magic C18 100Å 3 μ m PM3/66100/00 from Michrom). An UltiMate 3000 binary pump (Thermo Scientific) was used to generate the HPLC gradient as follows: 0-5% B in 15 min, 5-40% B in 35 min, 40-100% B in 20 min (A: 0.1% formic acid in water; B: 0.1% formic acid in acetonitrile). The eluted proteins were sprayed into a Q Exactive mass spectrometer (Thermo Scientific) equipped with a nano-ESI ion source. The mass spectrometer was operated in the information-dependent mode one MS scan followed by fifteen MS/MS scans for each cycle. Database searches were performed using an in-house Mascot server (Matrix Science) and performed against the International Protein Index (IPI) mouse database. Carbamidomethyl was set as a fixed modification while methionine oxidation and diglycine-modified lysine were set as variable modifications.

An electronic file containing all identified proteins from each gel slice shown in Supplementary Figure 9, along with data for corresponding gel slices from negative control lanes, is available upon request.

Klhl40 co-immunoprecipitation (co-IP) with Neb_{frag} and Lmod3. A total of 2 μ g containing a combination of FLAG-Klhl40, pcDNA3.1(+)/myc/His A (“EMPTY”), Lmod3-myc, and/or Neb_{frag}-myc was combined with Fugene 6 at a 3:1 DNA ratio to Fugene 6 and then added to 80-90% confluent COS7 cells in 6-well plates. 48 hours post-transfection, cells were washed with PBS and then scraped into PBS and transferred to 1.5mL microcentrifuge tubes. Collected cells were pelleted at 2,000xg for 3 minutes at

4°C. The supernatant was discarded and cells were resuspended and left on ice for at least 10 minutes in FLAG lysis buffer (50mM Tris pH 8.0, 137mM NaCl, 1mM EDTA, 10% glycerol, and 10mM NaF) with 1% Triton X-100, cOmplete mini EDTA protease inhibitor cocktail, and PhosSTOP phosphatase inhibitor cocktail. Lysate was centrifuged at 20,817xg for 15 min at 4°C. The insoluble pellet was discarded while the supernatant was retained.

To immunoprecipitate protein, 1µL of c-Myc antibody (Life Technologies) was added to 1mg of protein diluted to 1mL in FLAG lysis buffer with 1% TX-100 which was incubated overnight at 4°C. The following day, 50µL of washed Dynabeads Protein G (Life Technologies), were added to each immunoprecipitation reaction and incubated at 4°C for at least 2 hours. Beads were washed and pelleted using a magnetic stand (Invitrogen). The supernatant was discarded and the beads were boiled in 1X Laemmli buffer with 5% β-mercaptoethanol. The beads were pelleted and the supernatant was loaded onto a 4-20% Mini-PROTEAN TGX gel (Bio-Rad). For input lanes, original COS7 cell lysate was mixed with one volume of 2X Laemmli buffer with 5% β-mercaptoethanol was used. Following electrophoresis, standard Western blot analysis was performed (see below).

Klh140 stabilization of Neb_{frag} and Lmod3 and proteasomal analysis. A total of 2µg of DNA containing a combination of FLAG-Klh140, p3XFLAG-CMV-10-NHA (“EMPTY”), Lmod3-myc, and/or Neb_{frag}-myc was combined with Fugene 6 at a 3:1 DNA ratio to Fugene 6 and then added to 80-90% confluent COS7 cells in 6-well plates. 24 hours post-transfection, growth media containing either 0.1% DMSO (vehicle) or 10µM MG132

(APExBIO) in 0.1% DMSO was added to cells. 48 hours post-transfection, cells were washed with PBS and then scraped into 1mL of PBS and transferred to 1.5mL microcentrifuge tubes. Collected cells were pelleted at 2,000xg for 3 minutes at 4°C, and then resuspended in 1mL of PBS. Each tube was then split into two 500µL volumes and then pelleted again as before. RNA was extracted from one set of cells using TRIZOL according to manufacturer's instructions. Protein was extracted from the other set of cells and then loaded onto a 4-20% Criterion TGX gel (Bio-RAD) in the same manner stated in the previous section. Following electrophoresis, standard Western blot analysis was performed (see below).

Ubiquitination analysis of *Neb_{frag}* and *Lmod3*. A total of 12µg containing a combination of Lmod3-myc and p3XFLAG-CMV-10-NHA ("EMPTY") or FLAG-KIhl40 was transfected into COS7 cells on 10cm dishes in the same manner stated in the previous section. Proteasome inhibitor was added in the same manner as was stated before for in the proteasomal analysis section. Protein was collected from by washing cells and then collecting them into 5mL PBS by scraping cells with a sterile cell lifter. Cells were pelleted at 2,000xg for 3 min 4°C, resuspended in 1mL PBS, transferred to a microcentrifuge tube, and pelleted again. The supernatant was discarded and cells were lysed with 50µL FLAG lysis buffer with 1% Triton X-100 and 6M urea. 6M urea was used to disrupt protein-protein interactions to prevent co-immunoprecipitation of Lmod3-myc with FLAG-KIhl40. Lysate was diluted with 950µL FLAG lysis buffer with 1% Triton X-100 to bring the final concentration of urea to 0.3M. Insoluble cell debris was pelleted and discarded while the supernatant was retained.

To immunoprecipitate ubiquitinated protein, 5 μ L of K48 anti-ubiquitin antibody (Apu2; EMD Millipore) was added to 1.5mg of protein diluted to 500 μ L with FLAG lysis buffer with 1% Triton X-100 and 0.3M urea, and then diluted again with 500 μ L of FLAG lysis buffer with 1% Triton X-100 bringing the total urea concentration to 0.15M. Subsequent immunoprecipitation steps and Western analysis were performed in the same manner as the co-immunoprecipitation experiment in the previous section.

Neb_{frag} and Lmod3 stabilization with Kihl40 domain deleted protein. To generate domain deletions of Kihl40, PCR gene splicing by overlap extension (PCR SOEing) was utilized (8). Designated Kihl40 deletion constructs (in red) were generated by splicing the following regions (numbers correspond to nucleotides in NCBI reference sequence NM_028202.3): **-BTB**: 170-235 with 545-2035; **-BACK**: 170-565 with 881-2035; **-KR**: 170-1246 with 2009-2035, **-BTB -KR**: 170-235 with 545-1246 and 2009-2035; **-BACK -KR**: 170-565 with 881-1246 and 2009-2035; **-BTB -BACK**: 170-235 with 545-565 and 881-2035; **-BTB -BACK -KR**: 170-235 with 545-565, 881-1246, and 2009-2035. All deletions were cloned into the p3XFLAG-CMV-10-NHA vector with the same endogenous Kozak sequence and translational stop site as 3XFLAG-HA-Kihl40.

To test the ability of each Kihl40 variant in stabilizing Neb_{frag} or Lmod3, cells were co-transfected with a total of 2 μ g of DNA containing a combination of Neb_{frag}-myc and Lmod3-myc with p3XFLAG-CMV-10-NHA ("EMPTY"), 3X-FLAG-HA-Kihl40 ("FL"), or one of the seven domain deletion variants of Kihl40 in the same manner as the co-immunoprecipitation experiment. RNA and protein were simultaneously extracted and

analyzed in the same manner as the first experiment to test the stabilization of Neb_{frag} and Lmod3 with Kihl40.

Western blot analysis. For all cell culture experiments, 25 μ g of protein was analyzed except for immunoprecipitated proteins whose final concentrations were not measured. For all Western analysis of tissue protein, 50 μ g of protein was used except for P1 mice where only 25 μ g of protein was used. To extract protein from tissues, tissues were disassociated in FLAG lysis buffer with 1% Triton X-100, cOmplete mini EDTA protease inhibitor cocktail, PhosSTOP phosphatase inhibitor cocktail, and 6M urea using a mini pestle followed by sonication. Tissue lysate was centrifuged at 20,817xg for 15 minutes at 4°C and the insoluble pellet was discarded. Protein was mixed with one volume of 2X Laemmli buffer with 5% β -mercaptoethanol as described before for cell culture protein lysates, and standard SDS-PAGE electrophoresis was performed. All protein was transferred to Immobilon-P PVDF membrane (EMD Millipore) using a Trans-Blot SD Semi-Dry Transfer Cell (Bio-Rad).

To probe for FLAG-Kihl40, 1:20,000 dilution of mouse monoclonal anti-FLAG M2 (Sigma) was used with a 1:20,000 dilution of goat anti-mouse HRP conjugated secondary antibody (Bio-Rad). To probe for Neb_{frag}-myc or Lmod3-myc, a 1:5000 dilution of mouse monoclonal c-Myc antibody (Life Technologies) was used with a 1:10,000 dilution of conjugated anti-mouse secondary antibody. GAPDH was analyzed with a 1:10,000 dilution of mouse anti-GAPDH antibody (EMD Millipore) followed by a 1:20,000 dilution of conjugated anti-mouse secondary antibody. To analyze Lmod3, a 1:10,000 dilution of rabbit anti-Lmod3 (14948-1-AP, Proteintech) was used with a

1:10,000 dilution of goat anti-rabbit HRP conjugated secondary antibody (Bio-Rad). For cell culture and animal tissue protein analysis, all primary antibodies were incubated with blots for 1 hour at room temperature and overnight at 4°C, respectively, while secondary antibodies for both were incubated for 30 minutes at room temperature. All antibodies were diluted in 5% non-fat milk in TBS with 0.1% Tween-20 (5% milk/TBST).

Dot blot analysis of Neb and Gapdh. A Bio-Dot microfiltration apparatus (Bio-Rad) was used according to manufacturer instructions with a few exceptions. Protein in 15µL 1X Laemmli buffer with 2.5% β-mercaptoethanol was diluted with 285µL FLAG lysis buffer (no Triton), loaded onto the dot blot apparatus that contained a 0.45µm nitrocellulose membrane (Bio-Rad), and allowed to pass by gravity. Then, 500µL of TBS was loaded to each well and also allowed to pass by gravity. All subsequent steps involving the use of the apparatus were done based on manufacturer directions. Finally, the blot was removed from the apparatus and treated like a standard immunoblot. Neb and Gapdh were analyzed separately with a 1:1,000 dilution of rabbit anti-Neb antibody (19706-1-AP, ProteinTech) and 1:1,000 dilution of mouse anti-GAPDH antibody. Secondary antibodies were also used at a 1:1,000 dilution. Primary antibodies were incubated overnight at 4°C while secondary antibodies were incubated for 30 minutes at room temperature.

Quantitative proteomic analysis of skeletal muscle. Protein from quadriceps of P6 mice (3 WT and 3 KO) was extracted using Chemicon lysis buffer (50mM Tris-HCl [pH 6.8], 1mM EDTA, and 2% SDS) with cComplete mini EDTA protease inhibitor cocktail

and PhosSTOP phosphatase inhibitor cocktail. Tissue was disassociated in the same manner as described for Western blot analysis except everything was performed at room temperature to prevent SDS precipitation. To remove SDS, 500µg of protein was diluted in 100µL of the previous lysis buffer (including detergent, inhibitors, and urea) and then precipitated overnight at -20°C with six volumes of acetone pre-chilled to -20°C. Precipitated protein was pelleted by centrifugation at 8,000xg for 1 minute at 4°C and then washed three times with pre-chilled acetone. After washing, acetone was decanted, aspirated, and allowed to air dry for 10 minutes. Protein was resuspended in 100µL FLAG lysis buffer with 1% Triton X-100, cOmplete mini EDTA protease inhibitor cocktail, PhosSTOP phosphatase inhibitor cocktail, and 6M urea. 100µg of resuspended protein was then denatured, reduced, alkylated, and digested according to TMT Mass Tagging Kit (Thermo Scientific) directions. All six protein samples were labeled with the six available isobaric tags (WT: 126, 127 and 128; KO: 129, 130, and 131) also according to kit directions. Then, 30µL of labeled sample was combined into a single tube and then concentrated to approximately 20µL with a SpeedVac centrifuge (Thermo Scientific).

Approximately 50µg of TMT labeled peptides were loaded onto a 250µm (inner diameter [ID]) two-phase column containing a 5cm C18 reverse phase (RP) section packed with 3µm, 100Å, Luna C18 resin (Phenomenex) and upstream of a 2cm strong cation exchange (SCX) section, packed with 5µm, 100 Å Luna SCX resin (Phenomenex). Protein was desalted with Buffer A (0.1% formic acid) and then peptides were eluted from RP to SCX resin with Buffer B (80% acetonitrile in 0.1% formic acid).

Then, peptides were separated with a 75 μ m (ID) SCX 10cm column packed with 5 μ m, 100 Å Luna SCX resin using an Agilent 1200 HPLC system to generate the following gradient:

Time (min)	SCX Buffer A (%)	SCX Buffer B (%)	SCX Buffer C (%)
0	100	0	0
5	95	5	0
65	50	50	0
95	0	100	0
95.5	0	0	100
105	0	0	100
105.5	100	0	0
120	100	0	0

The SCX buffers used were: SCX Buffer A (7mM KH₂PO₄, 10% acetonitrile, pH 2.65), SCX Buffer B (7mM KH₂PO₄, 350mM KCl, pH 2.65), and SCX Buffer C (50 mM K₂HPO₄, pH 7.5). Each 5 min interval was treated as a single fraction. Each fraction of peptides was separated by an analytical capillary column (50 μ m X 17cm) packed with 5 μ m spherical C18 reversed phase material (YMC). A nanoAcquity UPLC system (Waters) was used to generate the following HPLC gradient: 0-30% B in 75 min, 30-70% B in 15 min, 70-90% B in 5 min (A = 0.1% formic acid in water, B = 0.1% formic acid in acetonitrile). The eluted peptides were sprayed into a LTQ ORBITRAP Velos mass spectrometer (ThermoFisher Scientific, San Jose, CA, USA) equipped with a nano-ESI ion source. The mass spectrometer was run in the same mode and searched the same database as stated for the tandem affinity purification experiment. The search parameters were: 7 ppm mass tolerance for precursor ions, 0.02 Da mass tolerance for product ions, with three missed cleavage sites allowed for trypsin digestion. Three variable modifications were included: protein N-Terminal acetylation, methionine oxidation, and cysteine carbamidomethylation. Two fixed modifications were include:

protein N-Terminal TMT6plex and lysine TMT6plex. The search results were filtered with both peptide significance threshold and expectation value to be below 0.05. The Mascot Percolator scores were used for all peptides. The quantitation method used was Proteome Sciences 6-plex Tandem Mass Tags(R) in Mascot 2.3.2 (Matrix Science).

Relative abundance of each protein was reported relative to 126 reporter ion signal and each signal was internally normalized using the Mascot average normalization method. WT signals (126, 127, and 128) and KO signals (129, 130, and 131) were averaged and statistical significance was calculated. In total, 3177 proteins were identified and 375 proteins had statistically significant changes ($P < 0.05$) between WT and KO groups. Statistically significant changed proteins are listed in Supplementary Table 2. Non-significant changes and any protein that was not reliably detected in all six samples are not reported. An electronic file detailing all proteins identified, their signals, and all other relevant mass spectrometric data are available upon request.

Immunoblot analysis of KLHL40 deficient patient muscle samples. Western blotting was performed on patient and healthy human control muscle biopsies as previously described (9). Dot blots for human samples were performed in the same manner as mouse samples.

For Western blot analysis on patient samples, a mouse monoclonal antibody to GAPDH (G8795, Sigma; 1:80,000) and rabbit polyclonal antibodies to KLHL40 (HPA024463, Sigma; 1:5,000) and Lmod3 (14948-1-AP, Proteintech; 1:10,000) were used. Anti-mouse HRP and anti-rabbit HRP secondary antibodies were both used at a

1:10,000 dilution. For dot blot analysis, mouse anti-GAPDH antibody (HPA024463, Sigma; 1:5,000) and rabbit anti-Neb antibody (19706-1-AP, ProteinTech; 1:1000), were used on separate blots and analyzed like before with a 1:1000 dilution of their respective HRP secondary antibodies.

Supplemental Tables

Supplemental Table 1. Up-regulated sarcomeric genes in P0 Kihl40 KO skeletal muscle as determined by microarray analysis.	
Gene	KO (Relative Abundance)
ANKRD2	6.94606422
CSRP3	2.868707867
CSRP3	2.807537769
CSRP3	2.752740704
MYH2	2.381745199
MYH1	2.25913063
STARS	2.15833446
NRAP	1.825833485
MYL2	1.759961637
NRAP	1.730111779
LMCD1	1.687224009
LMCD1	1.647132119
TCAP	1.613970532
TTID	1.607421585
LMCD1	1.57656356
TCAP	1.495413831
TNNI1	1.458172161
MYOZ2	1.425645414
FLNC	1.424441384
TPM3	1.403110823
PDLIM5	1.369172646
PDLIM3	1.360706011
TPM3	1.349502914
MYOZ2	1.345235747
TNNC1	1.284171717
MuRF1	1.25939414
DES	1.186887972
MYH1	1.150573325
MYH7	1.140898091
MYOM2	1.118857726
ACTN2	1.105697878

Supplemental Table 2. Changes in protein levels in Kih140 KO skeletal muscle as determined by quantitative proteomics				
Protein description	Accession number	^aKO AVG/WT AVG	log₂(KO AVG/WT AVG)	log₂(eMPAI)
^b Kbtbd5 Isoform 1 of Kelch repeat and BTB domain-containing protein	IPI00675649	0.105	-3.253	-0.556
Lmod3 Uncharacterized protein	IPI00755154	0.234	-2.098	-2.737
Myh4 Myosin-4	IPI00404837	0.254	-1.976	3.779
Pvalb Parvalbumin alpha	IPI00230766	0.306	-1.710	1.438
Mybph Myosin-binding protein H	IPI00109166	0.400	-1.320	-0.667
Serpina1e Alpha-1-antitrypsin 1-5	IPI00123927	0.411	-1.282	-0.201
Srprb Uncharacterized protein	IPI00987951	0.446	-1.165	0.807
Mybpc2 Myosin-binding protein C, fast-type	IPI00169994	0.468	-1.095	0.791
C3 Isoform Long of Complement C3 (Fragment)	IPI00323624	0.493	-1.021	-1.396
Actn3 Alpha-actinin-3	IPI00136701	0.497	-1.010	2.676
Hpx Hemopexin	IPI00128484	0.513	-0.964	-1.396
Myh13 Uncharacterized protein	IPI00468665	0.523	-0.935	0.496
Serpina1c Alpha-1-antitrypsin 1-3	IPI00123920	0.552	-0.858	-0.201
Neb Uncharacterized protein	IPI00720238	0.553	-0.855	0.575
Srcrb4d Scavenger receptor cysteine-rich domain-containing group B	IPI00756667	0.554	-0.853	-4.059
Hhatl Protein-cysteine N-palmitoyltransferase HHAT-like protein	IPI00315964	0.558	-0.843	-2.322
Apoc2 Apolipoprotein C-II	IPI00136266	0.576	-0.796	-1.599
Ighg Igh protein	IPI00556788	0.597	-0.744	-4.059
Plcl2 Inactive phospholipase C-like protein 2	IPI00322431	0.608	-0.718	-5.059
Tfrc Transferrin receptor protein 1	IPI00124700	0.663	-0.593	-2.644
Glt25d1 Procollagen galactosyltransferase 1	IPI00169870	0.664	-0.591	-3.322
Serpind1 Heparin cofactor 2	IPI00113227	0.686	-0.543	-4.059
Gamt Isoform 2 of Guanidinoacetate N-methyltransferase	IPI00136274	0.687	-0.541	-0.322
Itih4 inter alpha-trypsin inhibitor, heavy chain 4 isoform 2	IPI00119818	0.691	-0.534	-5.059
C2 Uncharacterized protein	IPI00114065	0.706	-0.502	-3.474
Igfbp5 Insulin-like growth factor-binding protein 5	IPI00114022	0.707	-0.500	-3.184
Myh8 Myosin-8	IPI00265380	0.713	-0.488	4.624
Igkv14-111 Anti-colorectal carcinoma light chain	IPI00462809	0.714	-0.486	-0.737
Rpl3l ribosomal protein L3-like isoform 1	IPI00944079	0.723	-0.468	-2.943
Cmb1 Carboxymethylenebutenolidase homolog	IPI00153373	0.732	-0.449	-0.377
Plod1 Procollagen-lysine,2-oxoglutarate 5-dioxygenase 1	IPI00127407	0.733	-0.449	-3.059
Serpina1b Alpha-1-antitrypsin 1-2	IPI00129755	0.740	-0.434	-0.014

Supplemental Table 2. Changes in protein levels in Kihl40 KO skeletal muscle as determined by quantitative proteomics				
Protein description	Accession number	^aKO AVG/ WT AVG	log₂(KO AVG/WT AVG)	log₂(eMPAI)
Tuba8 Tubulin alpha-8 chain	IPI00311175	0.741	-0.432	1.183
Aarsd1;1700113I22Rik Uncharacterized protein	IPI00648676	0.742	-0.430	-1.690
Serpinh1 Serpin H1	IPI00114733	0.743	-0.428	1.310
Ndufa11 NADH dehydrogenase [ubiquinone] 1 alpha subcomplex subunit	IPI00318645	0.750	-0.415	-2.120
Apoa4 Apolipoprotein A-IV	IPI00377351	0.752	-0.411	1.674
Mpst 3-mercaptopyruvate sulfurtransferase	IPI00604945	0.753	-0.409	-0.667
Smtn Uncharacterized protein	IPI00110089	0.753	-0.408	-1.322
Fdps Farnesyl pyrophosphate synthase	IPI00120457	0.754	-0.408	-1.943
P4ha2 Isoform IIb of Prolyl 4-hydroxylase subunit alpha-2	IPI00120100	0.754	-0.407	-2.059
Oat Ornithine aminotransferase, mitochondrial	IPI00129178	0.756	-0.403	-1.737
Nkiras1 NF-kappa-B inhibitor-interacting Ras-like protein 1	IPI00318589	0.757	-0.402	-2.837
ApoH Beta-2-glycoprotein 1	IPI00322463	0.757	-0.402	-2.556
Iitm2a Integral membrane protein 2A	IPI00122250	0.757	-0.401	-2.059
Gpd1 Glycerol-3-phosphate dehydrogenase [NAD ⁺], cytoplasmic	IPI00230185	0.763	-0.390	0.766
Afm Uncharacterized protein	IPI00130654	0.765	-0.386	-3.474
Col3a1 Collagen alpha-1(III) chain	IPI00129571	0.765	-0.386	-2.943
Apoc1 Apolipoprotein C-I	IPI00119676	0.766	-0.385	-0.415
Ppib Peptidyl-prolyl cis-trans isomerase B	IPI00135686	0.768	-0.380	-0.713
Serpina1d Alpha-1-antitrypsin 1-4	IPI00123924	0.769	-0.378	-0.667
Nenf Neudesin	IPI00132005	0.778	-0.362	-0.644
Serpinf1 Pigment epithelium-derived factor	IPI00331088	0.778	-0.362	-1.644
Ikbip Isoform 1 of Inhibitor of nuclear factor kappa-B kinase-interacting protein	IPI00120310	0.780	-0.359	-2.737
Alb Serum albumin	IPI00131695	0.782	-0.354	3.494
Gc Vitamin D-binding protein	IPI00126184	0.785	-0.349	-0.737
Afp Alpha-fetoprotein	IPI00113163	0.786	-0.348	2.296
Gstm2 Glutathione S-transferase Mu 2	IPI00228820	0.791	-0.338	-3.059
Rrbp1 Isoform 3 of Ribosome-binding protein 1	IPI00121149	0.799	-0.324	-0.943
2810405K02Rik Prostamide/prostaglandin F synthase	IPI00119094	0.804	-0.315	-0.889
Tnnc2 Troponin C, skeletal muscle	IPI00284119	0.805	-0.314	6.671
Cdkn1c Isoform KIP2a of Cyclin-dependent kinase inhibitor 1C	IPI00118931	0.805	-0.313	-1.644
Serping1 Plasma protease C1 inhibitor	IPI00122977	0.806	-0.311	-4.059
Igkv5-39 Anti-HIV-1 reverse transcriptase single-chain variable region	IPI00471297	0.812	-0.301	-3.059

Supplemental Table 2. Changes in protein levels in Kihl40 KO skeletal muscle as determined by quantitative proteomics				
Protein description	Accession number	^aKO AVG/WT AVG	log₂(KO AVG/WT AVG)	log₂(eMPAI)
Cog5 Conserved oligomeric Golgi complex subunit 5	IPI00223863	0.814	-0.296	-4.644
Dbn1 Isoform A of Drebrin	IPI00135475	0.825	-0.278	-1.474
Ppp1r3a Protein phosphatase 1 regulatory subunit 3A	IPI00342163	0.827	-0.273	-1.599
Crtap Cartilage-associated protein	IPI00111370	0.839	-0.254	-0.916
F2 Prothrombin (Fragment)	IPI00114206	0.855	-0.225	-4.322
Dnajc3 DnaJ homolog subfamily C member 3	IPI00459033	0.859	-0.219	-2.556
Cndp2 Cytosolic non-specific dipeptidase	IPI00315879	0.864	-0.210	-3.059
Prkar1a Uncharacterized protein	IPI00119575	0.868	-0.204	-0.786
Nudt2 Bis(5~-nucleosyl)-tetrphosphatase [asymmetrical]	IPI00135345	0.870	-0.201	-1.152
Sugt1 Suppressor of G2 allele of SKP1 homolog	IPI00408957	0.873	-0.196	-2.556
Acta1 Actin, alpha skeletal muscle	IPI00110827	0.875	-0.193	8.975
Vapb Vesicle-associated membrane protein-associated protein B	IPI00135655	0.876	-0.191	-1.322
Ssr4 Translocon-associated protein subunit delta	IPI00122346	0.878	-0.188	-0.014
Stx18 Isoform 1 of Syntaxin-18	IPI00112000	0.878	-0.187	-3.644
Tbcb Tubulin-folding cofactor B	IPI00315948	0.885	-0.176	-3.059
Galnt2 Isoform 1 of Polypeptide N-acetylgalactosaminyltransferase 2	IPI00420710	0.890	-0.168	-3.184
Zhx2 Zinc fingers and homeoboxes protein 2	IPI00399681	0.894	-0.162	-5.059
Ctsc Dipeptidyl peptidase 1	IPI00130015	0.908	-0.139	-4.059
Aif1l Allograft inflammatory factor 1-like	IPI00458418	0.923	-0.115	-2.474
Rpl23a;Gm10132 60S ribosomal protein L23a	IPI00461456	0.931	-0.103	-0.916
Reep5 receptor expression-enhancing protein 5	IPI00315463	0.958	-0.062	-1.644
Camk1 Calcium/calmodulin-dependent protein kinase type 1	IPI00130439	1.044	0.062	-2.644
6330577E15Rik Isoform 1 of Swi5-dependent recombination DNA rep:	IPI00458153	1.065	0.091	-3.474
Ddx39 Isoform 1 of ATP-dependent RNA helicase DDX39A	IPI00123878	1.071	0.099	-1.089
Ddx3x ATP-dependent RNA helicase DDX3X	IPI00230035	1.075	0.105	-0.340
Bphl Putative uncharacterized protein	IPI00320462	1.088	0.122	-2.252
Plxdc2 Plexin domain-containing protein 2	IPI00471179	1.091	0.126	-4.059
Atp5d ATP synthase subunit delta, mitochondrial	IPI00453777	1.098	0.135	1.422
Ndufa10 NADH dehydrogenase [ubiquinone] 1 alpha subcomplex subu	IPI00116748	1.107	0.147	-0.494
Echs1 Enoyl-CoA hydratase, mitochondrial	IPI00454049	1.109	0.149	0.934
Ndufb3 NADH dehydrogenase [ubiquinone] 1 beta subcomplex subuni	IPI00133403	1.110	0.151	-1.837
Xpnpep3 Isoform 2 of Probable Xaa-Pro aminopeptidase 3	IPI00221972	1.110	0.151	-3.644

Supplemental Table 2. Changes in protein levels in Kih140 KO skeletal muscle as determined by quantitative proteomics				
Protein description	Accession number	^aKO AVG/ WT AVG	log₂(KO AVG/WT AVG)	log₂(eMPAI)
Hmgb2 High mobility group protein B2	IPI00462291	1.111	0.152	-2.059
Hnrnp1 Heterogeneous nuclear ribonucleoprotein H	IPI00133916	1.112	0.153	1.111
Vdac1 Isoform Mt-VDAC1 of Voltage-dependent anion-selective chanr	IPI00230540	1.113	0.154	1.895
Mtx2 Metaxin-2	IPI00225254	1.114	0.156	-2.059
Cyb5r1 Isoform 1 of NADH-cytochrome b5 reductase 1	IPI00119131	1.116	0.158	-1.644
Aldh3a2 Aldehyde dehydrogenase	IPI00111235	1.116	0.158	-4.059
Coq7 Ubiquinone biosynthesis protein COQ7 homolog	IPI00125592	1.119	0.162	-1.000
Ptges3;LOC100048119;Gm9769 Prostaglandin E synthase 3	IPI00127989	1.120	0.163	-0.136
Ccdc56 Coiled-coil domain-containing protein 56	IPI00135208	1.121	0.165	-1.737
Phospho1 Phosphoethanolamine/phosphocholine phosphatase	IPI00153582	1.121	0.165	-3.059
2310003C23Rik Protein C20orf11 homolog	IPI00110487	1.123	0.167	-1.943
Tor1aip2 Torsin-1A-interacting protein 2	IPI00421157	1.123	0.167	-2.322
LOC100045848 protein BUD31 homolog isoform 2	IPI00849741	1.124	0.168	-1.322
Bola2 Isoform 1 of BolA-like protein 2	IPI00221694	1.126	0.171	-1.515
Ppa2 Isoform 1 of Inorganic pyrophosphatase 2, mitochondrial	IPI00127050	1.126	0.171	-1.889
Tbcc Tubulin-specific chaperone C	IPI00122348	1.127	0.172	-2.474
Tmpo Isoform Alpha of Lamina-associated polypeptide 2, isoforms alp	IPI00126338	1.129	0.175	-1.556
Suox Sulfite oxidase, mitochondrial	IPI00153144	1.130	0.177	-4.059
Tnxb Uncharacterized protein	IPI00130794	1.132	0.179	-1.737
Fen1 Putative uncharacterized protein	IPI00410836	1.132	0.179	-3.837
0610009D07Rik Pre-mRNA branch site protein p14	IPI00117687	1.139	0.188	-0.304
Spag7 Sperm-associated antigen 7	IPI00273232	1.140	0.189	-2.000
Cutc Copper homeostasis protein cutC homolog	IPI00112176	1.143	0.192	-3.059
2310022B05Rik Uncharacterized protein C1orf198 homolog	IPI00225267	1.146	0.196	-3.474
Ndufa4 NADH dehydrogenase [ubiquinone] 1 alpha subcomplex subur	IPI00125929	1.148	0.199	1.195
Mrpl11 39S ribosomal protein L11, mitochondrial	IPI00132470	1.148	0.199	-0.971
Nup153 nucleoporin 153	IPI00330624	1.149	0.201	-5.644
Ndufa2 NADH dehydrogenase [ubiquinone] 1 alpha subcomplex subur	IPI00315302	1.149	0.201	0.986
Mrps23 28S ribosomal protein S23, mitochondrial	IPI00284934	1.150	0.201	-0.269
Srsf4 Uncharacterized protein	IPI00606760	1.152	0.204	-2.556
Txnl1 Thioredoxin-like protein 1	IPI00266281	1.153	0.205	-0.667
Thoc4 Isoform 1 of THO complex subunit 4	IPI00114407	1.154	0.207	-0.286

Supplemental Table 2. Changes in protein levels in Kihl40 KO skeletal muscle as determined by quantitative proteomics				
Protein description	Accession number	^aKO AVG/ WT AVG	log₂(KO AVG/WT AVG)	log₂(eMPAI)
Vdac3 voltage-dependent anion-selective channel protein 3 isoform 1	IPI00991021	1.155	0.207	0.911
Bat3 Large proline-rich protein BAG6	IPI00130381	1.156	0.209	-2.396
Acad10 Acyl-CoA dehydrogenase family member 10	IPI00170013	1.158	0.212	-5.059
Afg3l2 AFG3-like protein 2	IPI00170357	1.159	0.213	-2.737
Lypla2 Acyl-protein thioesterase 2	IPI00123518	1.160	0.214	-1.786
Hnrnpr Putative uncharacterized protein	IPI00128441	1.160	0.215	-0.358
Srrt Isoform C of Serrate RNA effector molecule homolog	IPI00224644	1.163	0.217	-3.322
Uqcrcs1 Cytochrome b-c1 complex subunit Rieske, mitochondrial	IPI00133240	1.163	0.217	1.163
Cyc1 Isoform 1 of Cytochrome c1, heme protein, mitochondrial	IPI00132728	1.163	0.217	0.816
Naa38 N-alpha-acetyltransferase 38, NatC auxiliary subunit	IPI00263042	1.163	0.218	1.310
Rbm17 Splicing factor 45	IPI00170394	1.163	0.218	-3.837
Nup54 Nuclear pore complex protein Nup54	IPI00225192	1.164	0.219	-3.059
Mrps18b Isoform 1 of 28S ribosomal protein S18b, mitochondrial	IPI00118193	1.164	0.220	-2.000
6720456B07Rik Protein BRICK1	IPI00127176	1.166	0.222	-1.286
Peg3 Isoform 1 of Paternally-expressed gene 3 protein	IPI00330240	1.168	0.223	-4.644
Atp5e ATP synthase subunit epsilon, mitochondrial	IPI00230241	1.169	0.225	-0.943
Hibadh 3-hydroxyisobutyrate dehydrogenase, mitochondrial	IPI00116222	1.169	0.225	-0.837
Tsg101 Tumor susceptibility gene 101 protein	IPI00117944	1.169	0.225	-2.737
Ndufa3 NADH dehydrogenase [ubiquinone] 1 alpha subcomplex subunit	IPI00132216	1.170	0.227	-1.434
Erbp2ip Isoform 1 of Protein LAP2	IPI00454041	1.171	0.228	-5.644
Ndufa12 NADH dehydrogenase (Ubiquinone) 1 alpha subcomplex, 12	IPI00344004	1.171	0.228	0.014
Mrpl41 39S ribosomal protein L41, mitochondrial	IPI00378520	1.171	0.228	0.138
Mrpl23 39S ribosomal protein L23, mitochondrial	IPI00136310	1.172	0.229	-2.252
Atp1b4 Isoform A of Protein ATP1B4	IPI00117634	1.173	0.230	-1.059
Eif3j Uncharacterized protein	IPI00556700	1.173	0.230	-0.415
Aco2 Aconitate hydratase, mitochondrial	IPI00116074	1.173	0.230	1.541
Impa2 Inositol monophosphatase 2	IPI00126255	1.173	0.230	-2.120
Ptges2 Prostaglandin E synthase 2	IPI00312174	1.173	0.231	-0.059
2700060E02Rik UPF0568 protein C14orf166 homolog	IPI00132456	1.175	0.233	0.176
Rbm8a Isoform 2 of RNA-binding protein 8A	IPI00109860	1.175	0.233	0.227
Crk Isoform Crk-II of Adapter molecule crk	IPI00307991	1.177	0.235	-0.322
Nsfl1c Isoform 3 of NSFL1 cofactor p47	IPI00387232	1.177	0.236	0.070

Supplemental Table 2. Changes in protein levels in Kihl40 KO skeletal muscle as determined by quantitative proteomics				
Protein description	Accession number	^aKO AVG/ WT AVG	log₂(KO AVG/WT AVG)	log₂(eMPAI)
Nolc1 nucleolar and coiled-body phosphoprotein 1 isoform D	IPI00719871	1.178	0.236	-4.644
Parp3 Uncharacterized protein	IPI00625263	1.178	0.237	-4.322
Clpp Putative ATP-dependent Clp protease proteolytic subunit, mitoch	IPI00133270	1.180	0.238	-1.358
Fubp3 far upstream element (FUSE) binding protein 3	IPI00379513	1.181	0.240	-1.737
Cox4i1 Cytochrome c oxidase subunit 4 isoform 1, mitochondrial	IPI00117978	1.182	0.241	0.575
Gnao1 Isoform Alpha-2 of Guanine nucleotide-binding protein G(o) sul	IPI00115546	1.182	0.242	-2.556
Tra2b Isoform 1 of Transformer-2 protein homolog beta	IPI00139259	1.183	0.243	-3.184
Msi2 Isoform 1 of RNA-binding protein Musashi homolog 2	IPI00120924	1.183	0.243	-0.252
Scarb2 Lysosome membrane protein 2	IPI00127447	1.187	0.247	-4.059
Sf3b2 splicing factor 3b, subunit 2	IPI00349401	1.187	0.248	-3.322
Mrp12 39S ribosomal protein L12, mitochondrial	IPI00118963	1.188	0.249	-0.474
Comp Cartilage oligomeric matrix protein	IPI00127506	1.191	0.252	-4.644
Coq9 Ubiquinone biosynthesis protein COQ9, mitochondrial	IPI00169862	1.191	0.253	-0.690
D10Jhu81e;LOC100046684 ES1 protein homolog, mitochondrial	IPI00133284	1.192	0.253	-0.474
Aspn Asporin	IPI00117957	1.192	0.254	-0.396
Pgp Phosphoglycolate phosphatase	IPI00380195	1.193	0.255	-2.252
Nudt21 Cleavage and polyadenylation specificity factor subunit 5	IPI00132473	1.194	0.255	-1.889
Hspd1 Isoform 1 of 60 kDa heat shock protein, mitochondrial	IPI00308885	1.194	0.256	1.926
Cobl Isoform 1 of Protein cordon-bleu	IPI00330247	1.194	0.256	-3.837
Smug1 Single-strand selective monofunctional uracil DNA glycosylase	IPI00420346	1.195	0.257	-3.059
Phb Prohibitin	IPI00133440	1.196	0.258	1.632
Ppm1a Protein phosphatase 1A	IPI00114802	1.197	0.259	-1.120
Hspe1-rs1 MCG8024	IPI00120045	1.198	0.261	1.316
Park7 Protein DJ-1	IPI00117264	1.199	0.262	-0.286
Tubb2a Tubulin beta-2A chain	IPI00338039	1.199	0.262	3.770
Pgrmc2 Membrane-associated progesterone receptor component 2	IPI00351206	1.199	0.262	-0.494
Atp5k ATP synthase subunit e, mitochondrial	IPI00111770	1.199	0.262	0.782
H2afx Histone H2A.x	IPI00230264	1.199	0.262	2.516
Cfl2 Cofilin-2	IPI00266188	1.200	0.263	1.144
Tollip Toll-interacting protein	IPI00136618	1.200	0.263	-3.059
Tor1aip1 Lamina-associated polypeptide 1B	IPI00762273	1.200	0.263	-1.556
Hdh2 Isoform 1 of Haloacid dehalogenase-like hydrolase domain-cor	IPI00111166	1.201	0.264	-3.184

Supplemental Table 2. Changes in protein levels in KIf140 KO skeletal muscle as determined by quantitative proteomics				
Protein description	Accession number	^aKO AVG/WT AVG	log₂(KO AVG/WT AVG)	log₂(eMPAI)
Cenpv Isoform 1 of Centromere protein V	IPI00318428	1.202	0.266	-2.000
Pdha1 Pyruvate dehydrogenase E1 component subunit alpha, somatic	IPI00337893	1.203	0.267	0.506
Rtn4 Isoform 2 of Reticulon-4	IPI00270767	1.203	0.267	-0.737
Nedd8 NEDD8	IPI00127021	1.205	0.269	-0.269
Cpsf6 Cleavage and polyadenylation specificity factor subunit 6	IPI00421085	1.205	0.269	-2.396
Sdhb Succinate dehydrogenase [ubiquinone] iron-sulfur subunit, mitoc	IPI00338536	1.206	0.270	1.646
Pex14 Peroxisomal membrane protein PEX14	IPI00127237	1.206	0.270	-3.644
Cbx3;Gm10068 Chromobox protein homolog 3	IPI00129468	1.206	0.270	0.604
Letm1 LETM1 and EF-hand domain-containing protein 1, mitochondria	IPI00131177	1.207	0.272	-1.786
Chchd2 Coiled-coil-helix-coiled-coil-helix domain-containing protein 2,	IPI00284925	1.209	0.274	-2.120
Apobec2 Probable C->U-editing enzyme APOBEC-2	IPI00125150	1.209	0.274	0.926
Dlat Dihydrolipoyllysine-residue acetyltransferase component of pyruvate	IPI00153660	1.210	0.275	-0.269
Tufm Isoform 1 of Elongation factor Tu, mitochondrial	IPI00274407	1.212	0.277	1.214
Dci Enoyl-CoA delta isomerase 1, mitochondrial	IPI00114416	1.212	0.277	1.541
Nme1 Nucleoside diphosphate kinase A	IPI00131459	1.212	0.278	0.465
Plin5 Isoform 1 of Perilipin-5	IPI00226181	1.212	0.278	-1.690
Ube2d2 Ubiquitin-conjugating enzyme E2 D2	IPI00125135	1.212	0.278	-2.322
Hnrpd1 Heterogeneous nuclear ribonucleoprotein D-like	IPI00129417	1.213	0.278	-0.494
Dek Protein DEK	IPI00227720	1.213	0.279	-2.322
Hif1an Isoform 1 of Hypoxia-inducible factor 1-alpha inhibitor	IPI00652254	1.215	0.281	-2.556
Dlst Isoform 1 of Dihydrolipoyllysine-residue succinyltransferase comp	IPI00134809	1.217	0.283	-0.556
Jsrp1 Isoform 1 of Junctional sarcoplasmic reticulum protein 1	IPI00881120	1.217	0.284	-0.916
Gtf2f1 General transcription factor IIF subunit 1	IPI00153986	1.219	0.285	-3.184
Ndrp2 Isoform 1 of Protein NDRG2	IPI00136134	1.219	0.286	-0.120
Ccdc51 Isoform 1 of Coiled-coil domain-containing protein 51	IPI00110708	1.221	0.288	-2.644
Uqcrcq Cytochrome b-c1 complex subunit 8	IPI00224210	1.221	0.288	1.310
Cox6b1 Cytochrome c oxidase subunit 6B1	IPI00225390	1.221	0.288	2.101
LOC100504968;Ndufs5 NADH dehydrogenase [ubiquinone] iron-sulfur	IPI00117300	1.221	0.288	-0.105
Sspn Sarcospan	IPI00311020	1.222	0.289	-2.737
Sgcd Delta-sarcoglycan	IPI00124831	1.222	0.289	-0.690
Pdhb Pyruvate dehydrogenase E1 component subunit beta, mitochondria	IPI00132042	1.223	0.291	2.064
Klc4 Kinesin light chain 4	IPI00120089	1.229	0.297	-2.737

Supplemental Table 2. Changes in protein levels in Kihl40 KO skeletal muscle as determined by quantitative proteomics				
Protein description	Accession number	^aKO AVG/ WT AVG	log₂(KO AVG/WT AVG)	log₂(eMPAI)
Mtpn Myotrophin	IPI00228583	1.229	0.298	-0.862
Stam Putative uncharacterized protein	IPI00137731	1.230	0.298	-4.322
Sod1 Superoxide dismutase [Cu-Zn]	IPI00130589	1.230	0.298	0.687
Tcerg1 Isoform 2 of Transcription elongation regulator 1	IPI00229485	1.232	0.301	-3.644
Atp5h ATP synthase subunit d, mitochondrial	IPI00230507	1.233	0.302	1.257
Hnrnp2 Heterogeneous nuclear ribonucleoprotein H2	IPI00108143	1.234	0.303	0.651
Clip1 Isoform 1 of CAP-Gly domain-containing linker protein 1	IPI00123063	1.234	0.304	-2.120
Rpl17 60S ribosomal protein L17	IPI00453768	1.235	0.304	-0.578
Grb2 Isoform 1 of Growth factor receptor-bound protein 2	IPI00119058	1.235	0.305	-1.184
Endog Endonuclease G, mitochondrial	IPI00114840	1.236	0.306	-0.943
Srsf1 Isoform 1 of Serine/arginine-rich splicing factor 1	IPI00420807	1.238	0.308	1.202
Ndufs8 NADH dehydrogenase [ubiquinone] iron-sulfur protein 8, mitoc	IPI00170093	1.241	0.311	0.623
Gm10349;Nutf2 Nuclear transport factor 2	IPI00124149	1.242	0.313	0.454
Raph1 Uncharacterized protein	IPI00378430	1.246	0.317	-4.644
Ppif Peptidyl-prolyl cis-trans isomerase F, mitochondrial	IPI00116228	1.246	0.317	-2.737
Ube2g2 Putative uncharacterized protein	IPI00153094	1.246	0.318	-3.322
Cdv3 Isoform 2 of Protein CDV3	IPI00187275	1.248	0.319	0.791
C1qbp complement component 1 Q subcomponent-binding protein, m	IPI00132799	1.250	0.322	1.454
Actn2 alpha-actinin-2	IPI00387557	1.252	0.324	3.668
Vcl Vinculin	IPI00405227	1.252	0.324	1.021
Tmpo Isoform Epsilon of Lamina-associated polypeptide 2, isoforms b	IPI00466738	1.255	0.328	0.098
Fam136a Protein FAM136A	IPI00133411	1.258	0.331	-0.377
Bin1 Isoform 1 of Myc box-dependent-interacting protein 1	IPI00114352	1.258	0.331	1.021
Kif1b Isoform 3 of Kinesin-like protein KIF1B	IPI00130390	1.263	0.337	-3.837
Cecr5 Cat eye syndrome critical region protein 5 homolog	IPI00314106	1.264	0.338	-2.644
Pebp1 Phosphatidylethanolamine-binding protein 1	IPI00137730	1.265	0.339	2.039
Ndufv2 Isoform 1 of NADH dehydrogenase [ubiquinone] flavoprotein 2	IPI00169925	1.266	0.340	1.803
Ahsg Alpha-2-HS-glycoprotein	IPI00128249	1.269	0.343	-0.234
Tgfb2 Transforming growth factor beta-2	IPI00114180	1.271	0.346	-3.837
Uqcrh Cytochrome b-c1 complex subunit 6, mitochondrial	IPI00129516	1.275	0.350	3.948
Synpo2l Synaptopodin 2-like protein	IPI00226219	1.275	0.351	-0.415
Hint2 Histidine triad nucleotide-binding protein 2, mitochondrial	IPI00133034	1.276	0.351	-1.184

Supplemental Table 2. Changes in protein levels in Kih140 KO skeletal muscle as determined by quantitative proteomics				
Protein description	Accession number	^aKO AVG/WT AVG	log₂(KO AVG/WT AVG)	log₂(eMPAI)
Dbi Acyl-CoA-binding protein	IPI00667117	1.278	0.353	1.333
Tceal5 Transcription elongation factor A protein-like 5	IPI00228674	1.279	0.355	-0.578
Ppie Peptidyl-prolyl cis-trans isomerase E	IPI00111343	1.279	0.355	-3.474
Rbmxrt Heterogeneous nuclear ribonucleoprotein G-like 1	IPI00663587	1.282	0.359	0.263
Etfa Electron transfer flavoprotein subunit alpha, mitochondrial	IPI00116753	1.283	0.359	1.753
Rap2b Ras-related protein Rap-2b	IPI00138716	1.283	0.359	-1.515
Limd2 LIM domain-containing protein 2	IPI00221562	1.283	0.359	-2.184
Smpx Small muscular protein	IPI00120248	1.283	0.360	-0.322
Timm13 Mitochondrial import inner membrane translocase subunit Tim	IPI00134484	1.286	0.363	1.064
Akap1 Isoform 3 of A-kinase anchor protein 1, mitochondrial	IPI00115506	1.288	0.365	-3.837
Glrx5 Glutaredoxin-related protein 5, mitochondrial	IPI00378120	1.288	0.365	-2.252
Ech1 Delta(3,5)-Delta(2,4)-dienoyl-CoA isomerase, mitochondrial	IPI00130804	1.288	0.365	0.678
Anxa11 Annexin A11	IPI00124264	1.290	0.367	1.356
Timm8a1 Mitochondrial import inner membrane translocase subunit Ti	IPI00125776	1.291	0.368	0.322
Gm1614 hypothetical protein LOC381148	IPI00653542	1.294	0.372	-5.059
Ppp1r12b Uncharacterized protein	IPI00665734	1.294	0.372	-1.000
Mrps18a 28S ribosomal protein S18a, mitochondrial	IPI00320963	1.299	0.377	-2.837
Uqcrb Uncharacterized protein	IPI00132347	1.299	0.377	2.491
Etfb Electron transfer flavoprotein subunit beta	IPI00121440	1.300	0.379	2.141
Lym5 LYR motif-containing protein 5	IPI00471097	1.301	0.379	-1.786
Mtx1 metaxin-1 isoform 1	IPI00112327	1.302	0.381	-2.252
Lym7 Uncharacterized protein	IPI00117832	1.303	0.382	-2.252
Tppp3 Tubulin polymerization-promoting protein family member 3	IPI00133557	1.306	0.385	1.316
Acot13 Acyl-coenzyme A thioesterase 13	IPI00132958	1.308	0.388	-1.089
Hist1h2bj;Hist1h2bn;Hist1h2bf;Hist1h2bl Histone H2B type 1-F/J/L	IPI00114642	1.309	0.388	3.359
Tgoln2 Trans-Golgi network integral membrane protein 2	IPI00124572	1.311	0.390	-3.644
Myl1 Isoform MLC1 of Myosin light chain 1/3, skeletal muscle isoform	IPI00312700	1.313	0.392	8.213
Trim54 Tripartite motif-containing protein 54	IPI00319154	1.314	0.394	-1.434
Pacsin3 Protein kinase C and casein kinase II substrate protein 3	IPI00319933	1.316	0.397	-0.304
Plbd2 Isoform 1 of Putative phospholipase B-like 2	IPI00165730	1.317	0.397	-3.184
Mrpl2 39S ribosomal protein L2, mitochondrial	IPI00109740	1.319	0.400	-2.252
Tfam Isoform Mitochondrial of Transcription factor A, mitochondrial	IPI00112822	1.321	0.401	-1.515

Supplemental Table 2. Changes in protein levels in Kihl40 KO skeletal muscle as determined by quantitative proteomics				
Protein description	Accession number	^aKO AVG/ WT AVG	log₂(KO AVG/WT AVG)	log₂(eMPAI)
Gm20075;Btf3l4 Transcription factor BTF3 homolog 4	IPI00132539	1.324	0.404	-2.474
Filip1 Uncharacterized protein	IPI00756400	1.324	0.405	-3.474
Frg1 Protein FRG1	IPI00311968	1.325	0.406	-3.322
Pdk2 [Pyruvate dehydrogenase [lipoamide]] kinase isozyme 2, mitochondr	IPI00122251	1.327	0.408	-2.059
Shisa4 Protein shisa-4	IPI00228025	1.331	0.412	-2.556
Mavs Mitochondrial antiviral-signaling protein	IPI00122075	1.335	0.417	-1.434
Pycrl Pyrroline-5-carboxylate reductase 3	IPI00153234	1.339	0.421	-1.943
Pnpo Pyridoxine-5--phosphate oxidase	IPI00129096	1.339	0.422	-3.184
Hadha Trifunctional enzyme subunit alpha, mitochondrial	IPI00223092	1.345	0.428	1.683
Usf1 Upstream stimulatory factor 1	IPI00117062	1.352	0.435	-2.252
Sgcg Gamma-sarcoglycan	IPI00110503	1.353	0.436	-1.000
Stx16 syntaxin-16 isoform d	IPI00225880	1.353	0.436	-2.322
Sorbs2 Uncharacterized protein	IPI00177047	1.358	0.441	-2.837
Spry2 Protein sprouty homolog 2	IPI00135613	1.358	0.442	-3.322
Ywhag 14-3-3 protein gamma	IPI00230707	1.359	0.443	2.064
Mlf2 Myeloid leukemia factor 2	IPI00116372	1.361	0.444	-2.943
Prpf40b Isoform 3 of Pre-mRNA-processing factor 40 homolog B	IPI00377927	1.367	0.451	-5.059
B230120H23Rik Isoform 2 of Mitogen-activated protein kinase kinase	IPI00265705	1.375	0.459	-1.837
Sod2 Superoxide dismutase [Mn], mitochondrial	IPI00109109	1.375	0.460	-1.152
Mlycd Isoform Mitochondrial of Malonyl-CoA decarboxylase, mitochondr	IPI00114866	1.377	0.462	-2.943
N6amt1 N6-DNA methyltransferase A isoform 1	IPI00347285	1.378	0.463	-1.599
A230046K03Rik WASH complex subunit 7	IPI00831049	1.378	0.463	-5.644
Tacc2 transforming acidic coiled-coil-containing protein 2 isoform c	IPI00465585	1.383	0.467	-2.737
Pdlim5 Isoform 2 of PDZ and LIM domain protein 5	IPI00415684	1.390	0.475	1.043
Stk4 Serine/threonine-protein kinase 4	IPI00119772	1.399	0.484	-4.059
Cabc1 Isoform 1 of Chaperone activity of bc1 complex-like, mitochondr	IPI00122554	1.402	0.487	-0.474
Ldb3 Isoform 4 of LIM domain-binding protein 3	IPI00656173	1.411	0.497	2.070
Dnajb4 DnaJ homolog subfamily B member 4	IPI00110760	1.414	0.500	-0.713
Ccdc6 Uncharacterized protein	IPI00381495	1.415	0.501	-4.059
Coro6 Isoform B of Coronin-6	IPI00263646	1.416	0.502	-4.059
Pcmt1 Isoform 1 of Protein-L-isoaspartate(D-aspartate) O-methyltrans	IPI00329913	1.418	0.504	-1.152
Acsf2 Acyl-CoA synthetase family member 2, mitochondrial	IPI00122633	1.431	0.517	-3.322

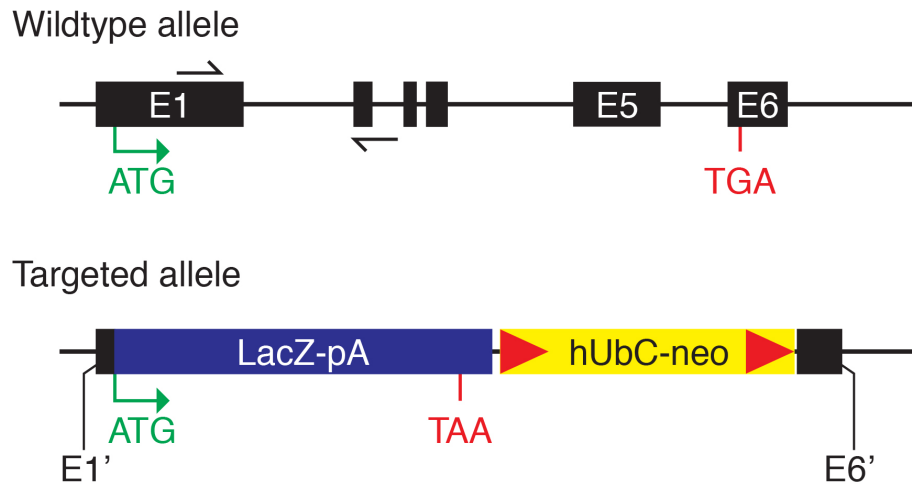
Supplemental Table 2. Changes in protein levels in Kih140 KO skeletal muscle as determined by quantitative proteomics				
Protein description	Accession number	^aKO AVG/ WT AVG	log₂(KO AVG/WT AVG)	log₂(eMPAI)
Svil Supervillin	IPI00170232	1.433	0.519	-2.644
Papln Papilin	IPI00110468	1.434	0.520	-5.059
Ablim1 Uncharacterized protein	IPI00169851	1.440	0.526	-4.644
Sorbs1 sorbin and SH3 domain-containing protein 1 isoform 1	IPI00125895	1.444	0.530	-1.556
Nmnat3 Nicotinamide mononucleotide adenylyltransferase 3	IPI00115459	1.451	0.537	-3.059
Diablo Diablo homolog, mitochondrial	IPI00120937	1.461	0.547	-3.059
Obscn obscurin isoform 2	IPI00915477	1.463	0.549	-1.396
Fhl1 Isoform 1 of Four and a half LIM domains protein 1	IPI00309997	1.476	0.561	0.526
Sgcb Beta-sarcoglycan	IPI00124836	1.476	0.562	-1.690
Synpo2 Isoform 1 of Synaptopodin-2	IPI00130162	1.478	0.563	-1.218
Cd36 Platelet glycoprotein 4	IPI00331214	1.478	0.563	-1.252
Rras Ras-related protein R-Ras	IPI00114594	1.482	0.567	-0.059
Asrgl1 L-asparaginase	IPI00223875	1.484	0.570	-1.690
Cdh13 Cadherin-13	IPI00123746	1.490	0.575	-2.474
Tcap Telethonin	IPI00119331	1.508	0.593	-0.578
Ccdc134 Isoform 1 of Coiled-coil domain-containing protein 134	IPI00226901	1.510	0.595	-3.059
Hspb1 Isoform A of Heat shock protein beta-1	IPI00128522	1.510	0.595	2.167
Xirp2 Isoform 1 of Xin actin-binding repeat-containing protein 2	IPI00353672	1.516	0.600	-3.474
Atp1b1 Sodium/potassium-transporting ATPase subunit beta-1	IPI00121550	1.522	0.606	-1.786
Des Desmin	IPI00130102	1.535	0.618	3.705
Lmna Isoform A of Prelamin-A/C	IPI00620256	1.541	0.623	2.441
Bag3 BAG family molecular chaperone regulator 3	IPI00331334	1.587	0.666	-0.201
Sms;Gm14680 Spermine synthase	IPI00124127	1.588	0.667	-1.515
Nrap Isoform 1 of Nebulin-related-anchoring protein	IPI00135182	1.599	0.678	-2.252
Fabp3 Fatty acid-binding protein, heart	IPI00230124	1.604	0.682	1.531
3425401B19Rik hypothetical protein LOC100504518	IPI00461683	1.619	0.695	-4.644
Flnc Uncharacterized protein	IPI00664670	1.620	0.696	0.251
Qk Isoform 6 of Protein quaking	IPI00759871	1.661	0.732	-0.943
Myot Myotilin	IPI00120508	1.674	0.744	0.176
Lmcd1 LIM and cysteine-rich domains protein 1	IPI00124513	1.683	0.751	0.546
Synpo Isoform 3 of Synaptopodin	IPI00415558	1.688	0.755	-1.218
Hspb8 Heat shock protein beta-8	IPI00122428	1.696	0.762	-2.644

Supplemental Table 2. Changes in protein levels in Kihl40 KO skeletal muscle as determined by quantitative proteomics				
Protein description	Accession number	^aKO AVG/WT AVG	log₂(KO AVG/WT AVG)	log₂(eMPAI)
Rapgef1 Rap guanine nucleotide exchange factor (GEF) 1 isoform 3	IPI00330231	1.724	0.786	-5.059
Hrc histidine rich calcium binding protein	IPI00469542	1.730	0.791	1.091
Adprh1 [Protein ADP-ribosylarginine] hydrolase-like protein 1	IPI00221629	1.734	0.794	-1.396
Hspb7 Uncharacterized protein	IPI00556871	1.736	0.795	2.254
Myl6b Myosin light chain 6B	IPI00261638	1.807	0.853	1.390
Myh1 Myosin-1	IPI00380896	1.823	0.866	3.886
Pdlim1 PDZ and LIM domain protein 1	IPI00309768	1.834	0.875	1.595
Snrpa1 U2 small nuclear ribonucleoprotein A~	IPI00170008	1.839	0.879	-1.396
Dnaja4 DnaJ homolog subfamily A member 4	IPI00125454	1.874	0.906	-1.059
Igsf1 Isoform 1 of Immunoglobulin superfamily member 1	IPI00311803	1.875	0.907	-3.837
Hba-a1;Hba-a2 Putative uncharacterized protein	IPI00110658	1.952	0.965	6.496
Myoz2 Myozenin-2	IPI00122334	1.983	0.988	2.313
Slmap Isoform 5 of Sarcolemmal membrane-associated protein	IPI00121581	1.990	0.992	-2.000
Tceal7 Transcription elongation factor A protein-like 7	IPI00830692	2.001	1.001	3.425
Hspa1b Heat shock 70 kDa protein 1B	IPI00346073	2.044	1.032	-0.667
Xirp1 xin actin-binding repeat-containing protein 1	IPI00955386	2.046	1.033	0.111
Smtnl1 Smoothelin-like protein 1	IPI00117028	2.120	1.084	0.111
Abra Actin-binding Rho-activating protein	IPI00225763	2.481	1.311	-2.000
Pdk4 [Pyruvate dehydrogenase [lipoamide]] kinase isozyme 4, mitochondria	IPI00119431	2.887	1.529	-1.286
Cryab Alpha-crystallin B chain	IPI00138274	3.010	1.590	3.724
Csrp3 Cysteine and glycine-rich protein 3	IPI00118153	3.147	1.654	-0.434
Ankrd2 Ankyrin repeat domain-containing protein 2	IPI00124985	4.686	2.228	1.642

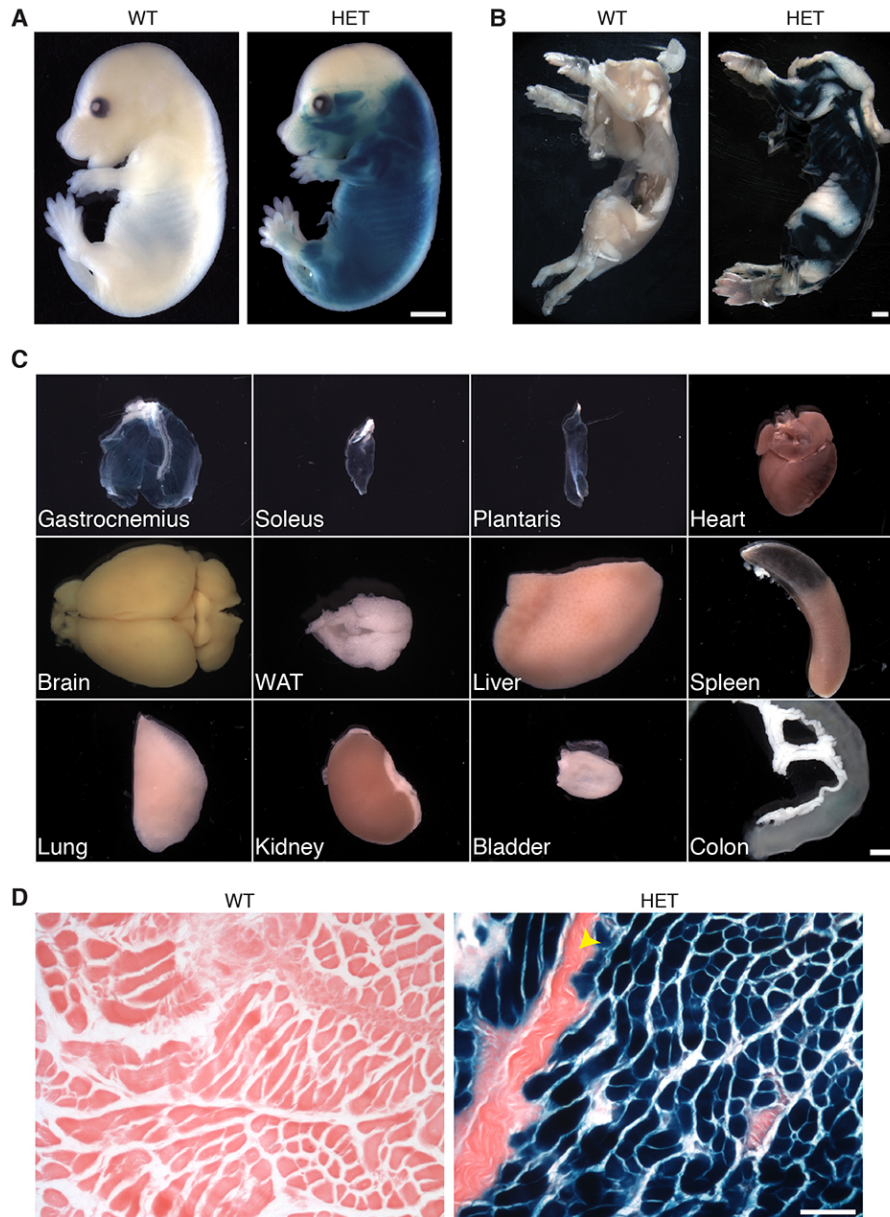
^aAverage KO signal/Average WT signal

^bKbtbd5 is an alternate name for Kihl40

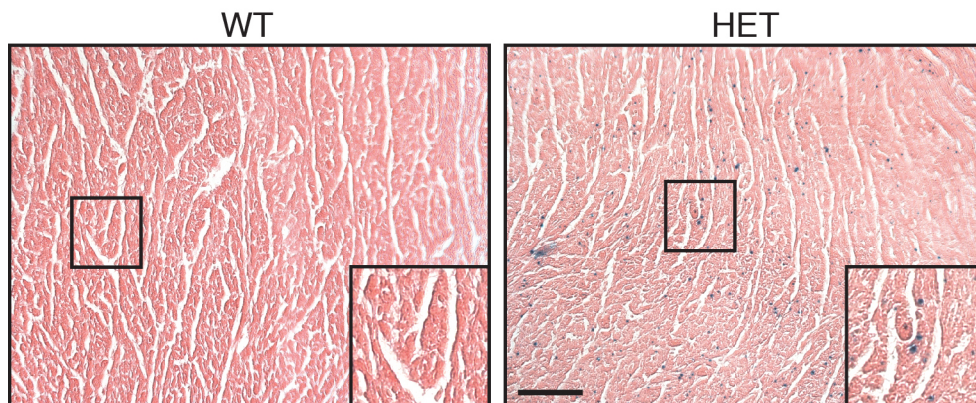
Supplemental Figures



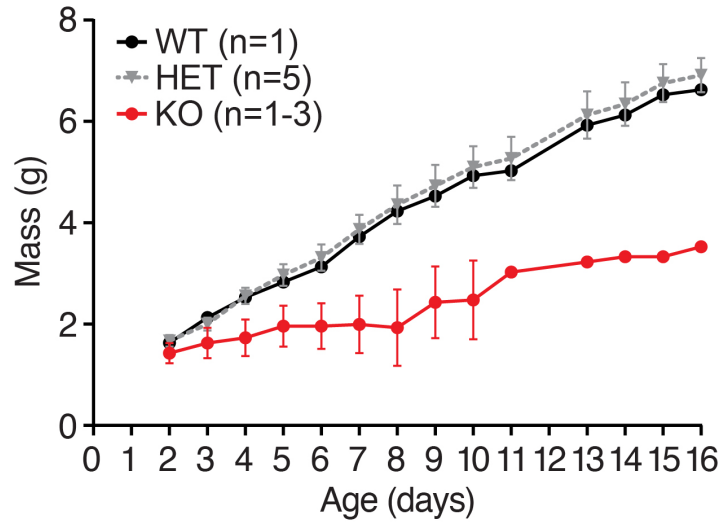
Supplemental Figure 1. Targeting strategy for *Khl40* knockout allele. The coding sequence of *Khl40* (not including the start codon) as well as 23 nucleotides past the stop codon (nucleotides 172-5816 of NCBI reference sequence NC_000075.6) were replaced with a β -galactosidase (LacZ-pA) and neomycin (hUbC-neo) expression cassette. The promoter and the 5' (E1') and 3' (E6') untranslated regions of *Khl40* were left intact allowing for LacZ expression to be driven by the endogenous promoter. Neomycin expression was driven by the human ubiquitin C (hUbC) promoter. Black boxes represent exons and half arrows indicate location of qPCR primers that were used to analyze *Khl40* mRNA. Red triangles denote loxP sites and ATG and TGA/TAA represent translational start and stop sites, respectively.



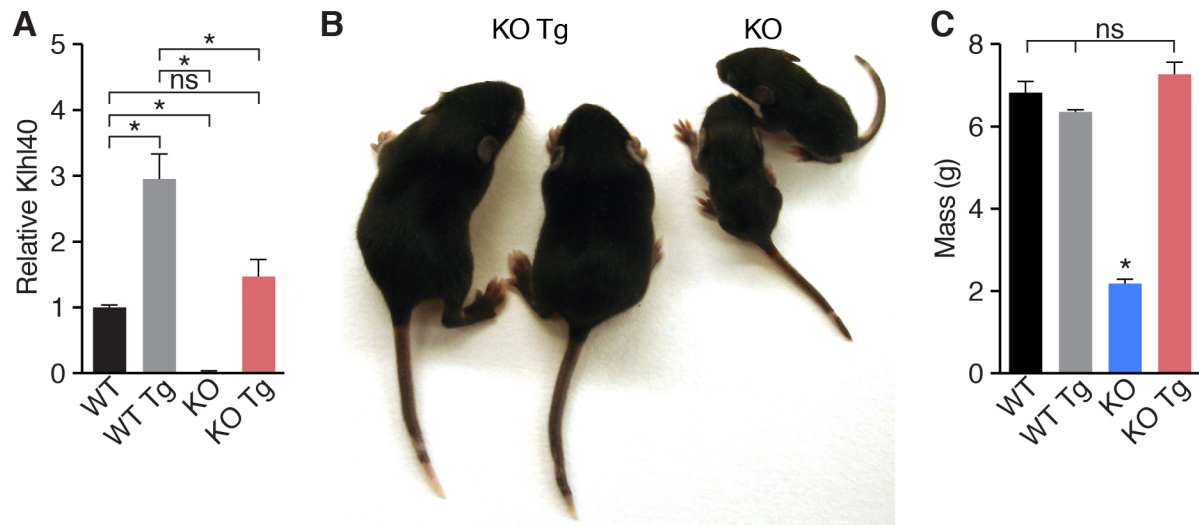
Supplemental Figure 2. *LacZ* knock-in into *Kihl40* locus shows muscle specific *lacZ* staining. (A, B) X-gal staining of *Kihl40* promoter driven *lacZ* reporter shows signal (blue stain) only in skeletal muscle of (A) HET E15 and (B) P8 mice, respectively. HET mice contain the knocked-in allele while WT mice lack the allele. (A, B) Scale bar: 1mm. (C) X-gal staining HET adult tissues also show muscle specific staining. Note that the black lesion on the spleen is due to a hemorrhage and not *lacZ* activity. Scale bar: 2mm. (D) X-gal stained sections of P8 muscle shows blue staining only in HET myofibers and not connective tissue (yellow arrowhead). Scale bar: 50 μ m.



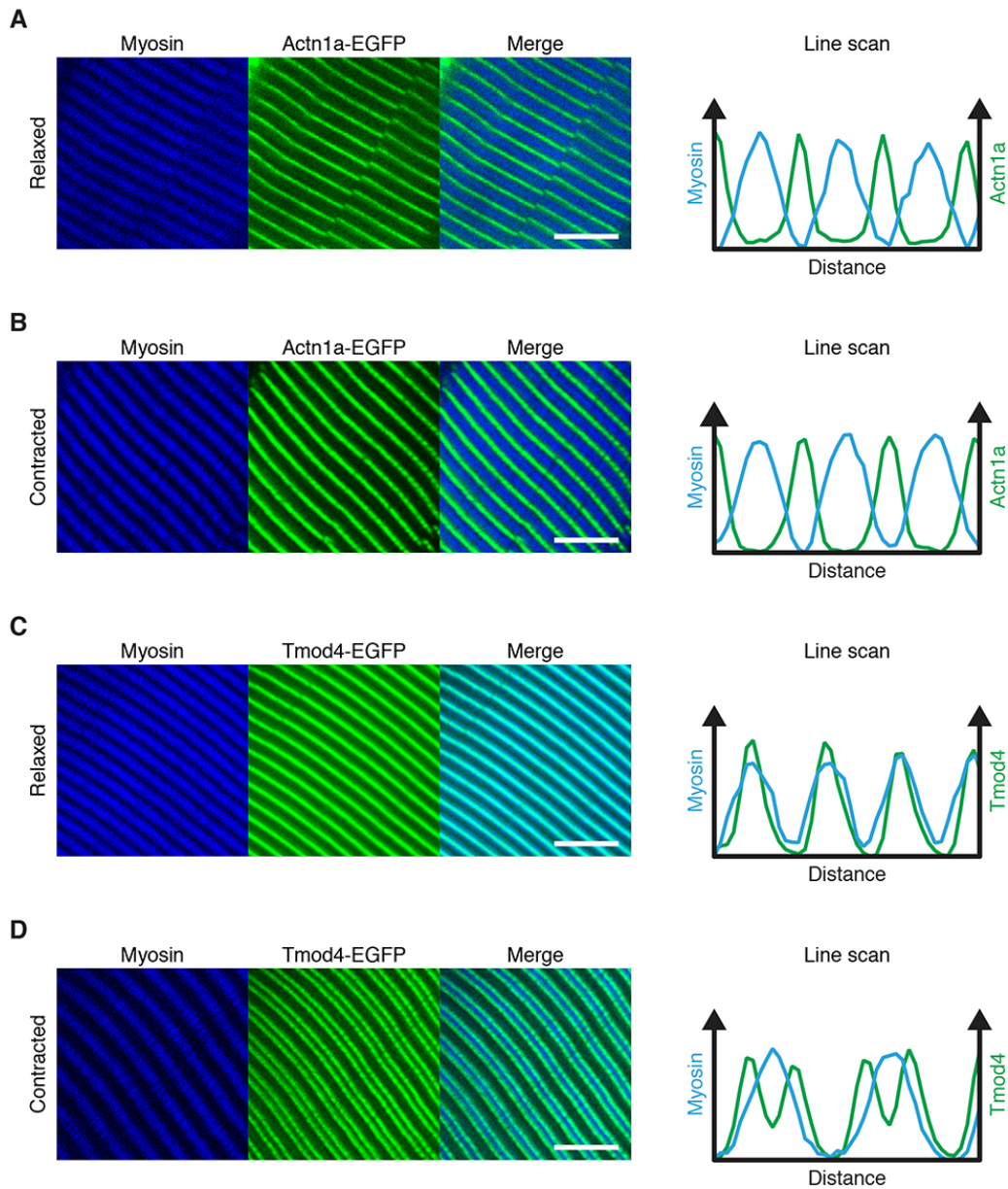
Supplemental Figure 3. Punctate lacZ staining in myocardium. X-gal staining in P8 heart sections of HET mice shows punctate blue staining, indicative of low lacZ reporter expression, that is absent in WT mice. Scale bar: 50 μ m. Boxed area is enlarged in inset.



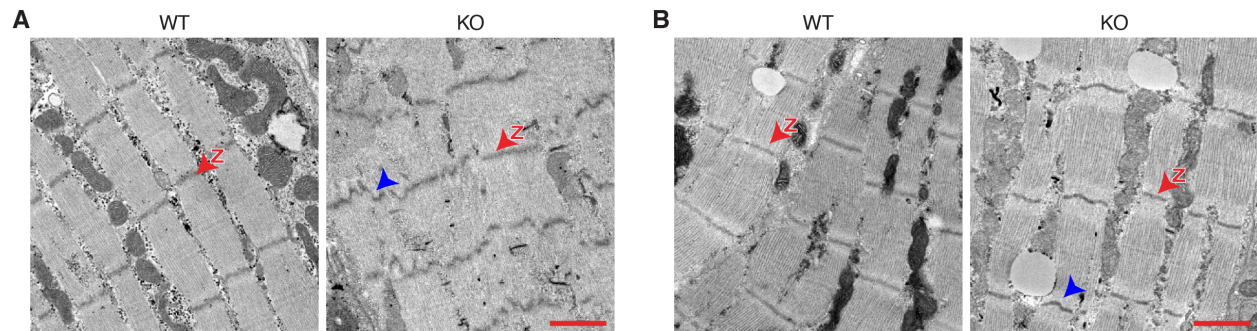
Supplemental Figure 4. Blunted growth of Khl40 KO mice. Khl40 mice show reduced growth within several days of birth. Number of animals for each genotype is indicated. KO mice numbers vary from 1-3 due to death of mice as time progressed.



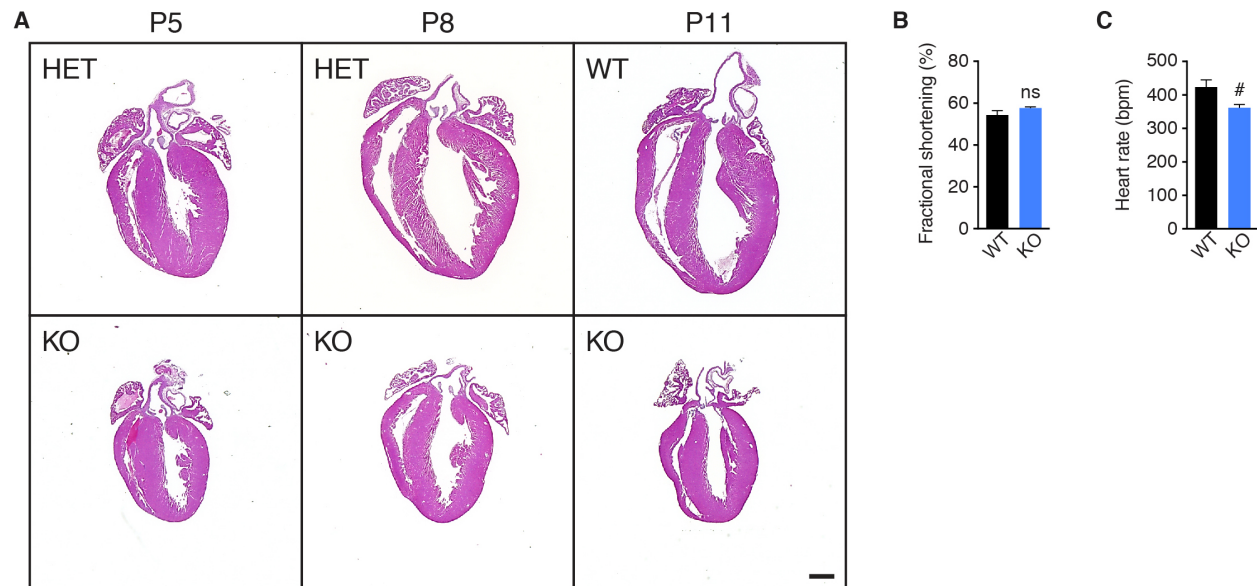
Supplemental Figure 5. Muscle-specific over-expression of *Kihl40* rescues *Kihl40* KO lethality. (A) qPCR analysis of *Kihl40* mRNA in P10 quadriceps of *Kihl40*^{+/+} (WT), *Kihl40*^{+/+};MCK-*Kihl40* (WT Tg), *Kihl40*^{-/-} (KO), and *Kihl40*^{-/-};MCK-*Kihl40* (KO Tg) mice shows approximately 3-fold overexpression of *Kihl40* in WT Tg mice. *Kihl40* transcript is restored to near-normal levels in KO Tg mice. N=3 for all genotypes. (B) Representative image of KO Tg and KO mice shows complete rescue of KO phenotype with muscle-specific overexpression of *Kihl40*. (C) Masses of KO Tg mice are indistinguishable from WT and WT Tg mice. WT n=5, WT Tg n=3, KO n=5, and KO Tg n=4. * statistically significant difference with a false discovery rate (FDR) of 0.05. Data are presented as mean ± SEM.



Supplemental Figure 6. Actn1a-EGFP and Tmod4-EGFP do not change localization in relaxed or contracted muscles. (A, B) Actn1a-EGFP and (C, D) Tmod4-EGFP localization relative to myosin visualized by second harmonic generation in (A, C) relaxed and (B, D) contracted muscles. (A, B) Actn1a-EGFP remains in the I-band while (B, D) Tmod4-EGFP remains in the A-band regardless of the contractile state of muscle. Note that Tmod4-EGFP appears as a doublet in contracted muscle likely due to hyper-contraction of sarcomeres that causes pointed ends of actin to run past each other over the M-line (10). Scale bar: 5 μ m.

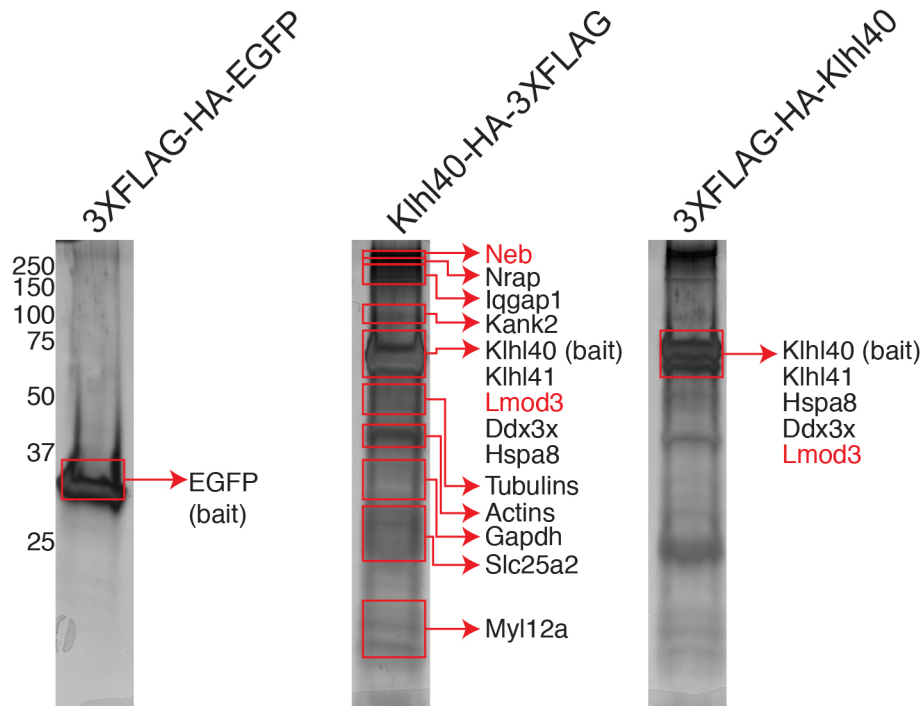


Supplemental Figure 7. P8 Kihl40 KO muscles show Z-line streaming, but P1 KO muscles are similar to WT. (A, B) EM analysis of longitudinal sections of (A) P8 diaphragm and (B) P1 diaphragms from WT and KO mice. (A, B) Red “Z”s with red arrowheads indicate representative Z-lines in each section. (A) Z-line streaming is apparent in P8 KO muscles (blue arrowhead). (B) P1 WT and KO muscles are comparable at P1 although subtle Z-line defects may be present (blue arrowhead). (A, B) Scale bar: 1 μ m.

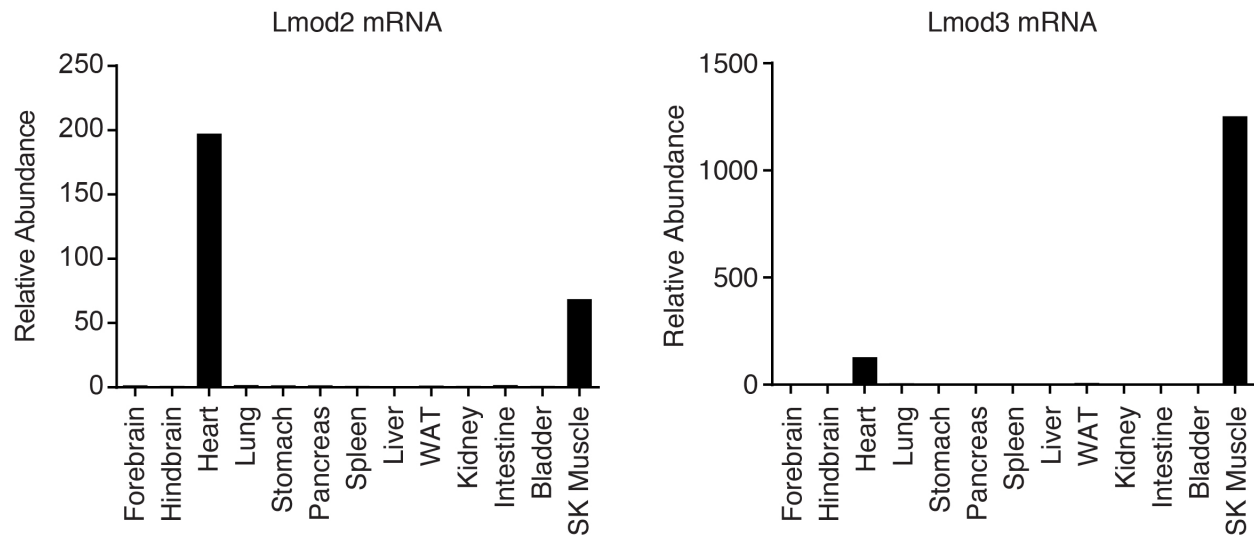


Supplemental Figure 8. *Kihl40* KO mice do not display any cardiac abnormalities.

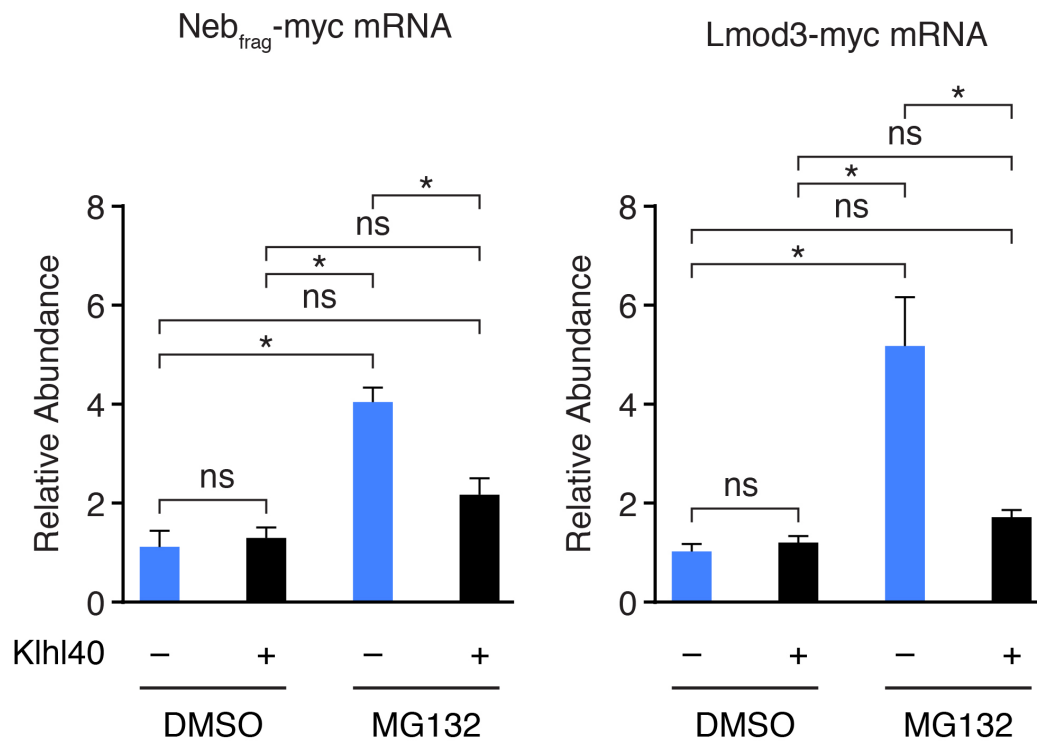
(A) P5, P8, and P11 hearts from HET, WT, or KO mice. KO hearts, though smaller, show no obvious signs of cardiac defects. Scale bar: 5mm. (B, C) P5 WT (n=3) and KO (n=6) (B) fractional shortening and (C) heart rate as determined by echocardiography. Fractional shortening is comparable between WT and KO, but heart rate is decreased 15% in KO mice. # $p < 0.05$. Data are presented as mean \pm SEM.



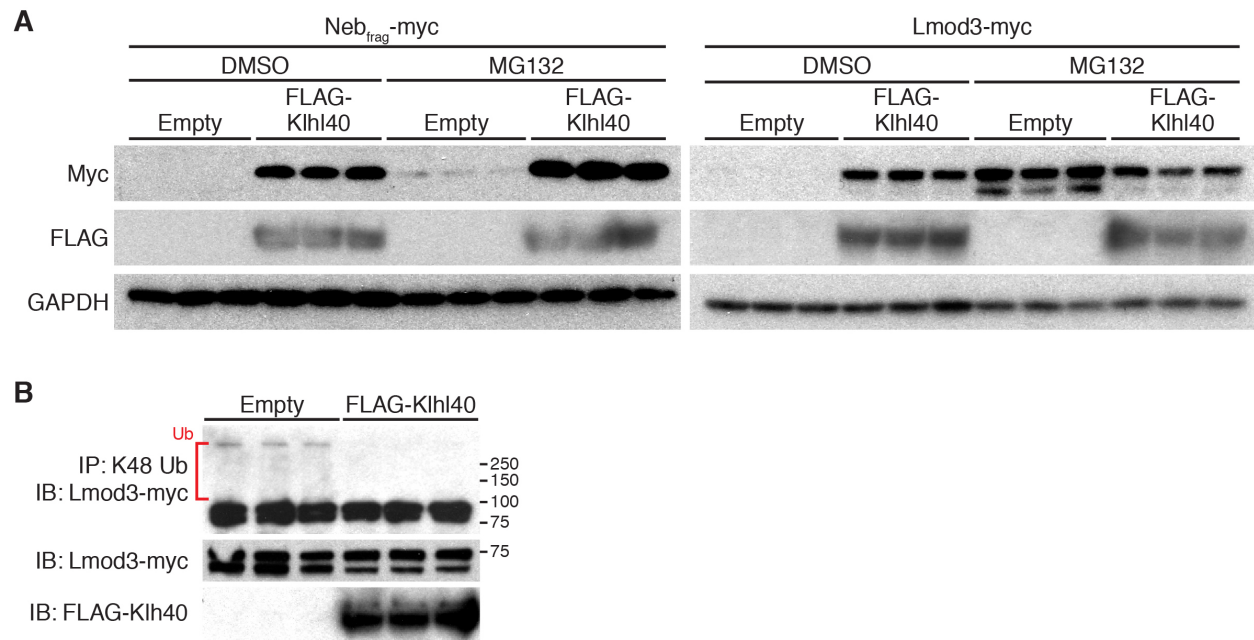
Supplemental Figure 9. Gel slices analyzed by mass spectrometry to identify Kihl40 binding partners. Representative silver stained gel of TAP protein from myotubes infected with 3XFLAG-HA-EGFP, Kihl40-HA-3XFLAG, or 3XFLAG-HA-Kihl40. Proteins listed next to each box indicate the most abundant protein(s) of the correct molecular weight identified in each corresponding area (data reproduced from Figure 4A). Abundance is based on estimated enrichment using exponentially modified protein abundance index (emPAI). All samples were ran on the same gel and are only separated to allow for labeling. Molecular weights for all three lanes are indicated on the left. Only a single region of the 3XFLAG-HA-Kihl40 lane differed from Kihl40-HA-3XFLAG, but mass spectrometric analysis identified the same proteins between both regions. The additional band in 3XFLAG-HA-Kihl40 could be a cleavage product of one of the identified proteins which will require additional analysis to determine. A list of all identified proteins with their corresponding mass spectrometric information is available upon request.



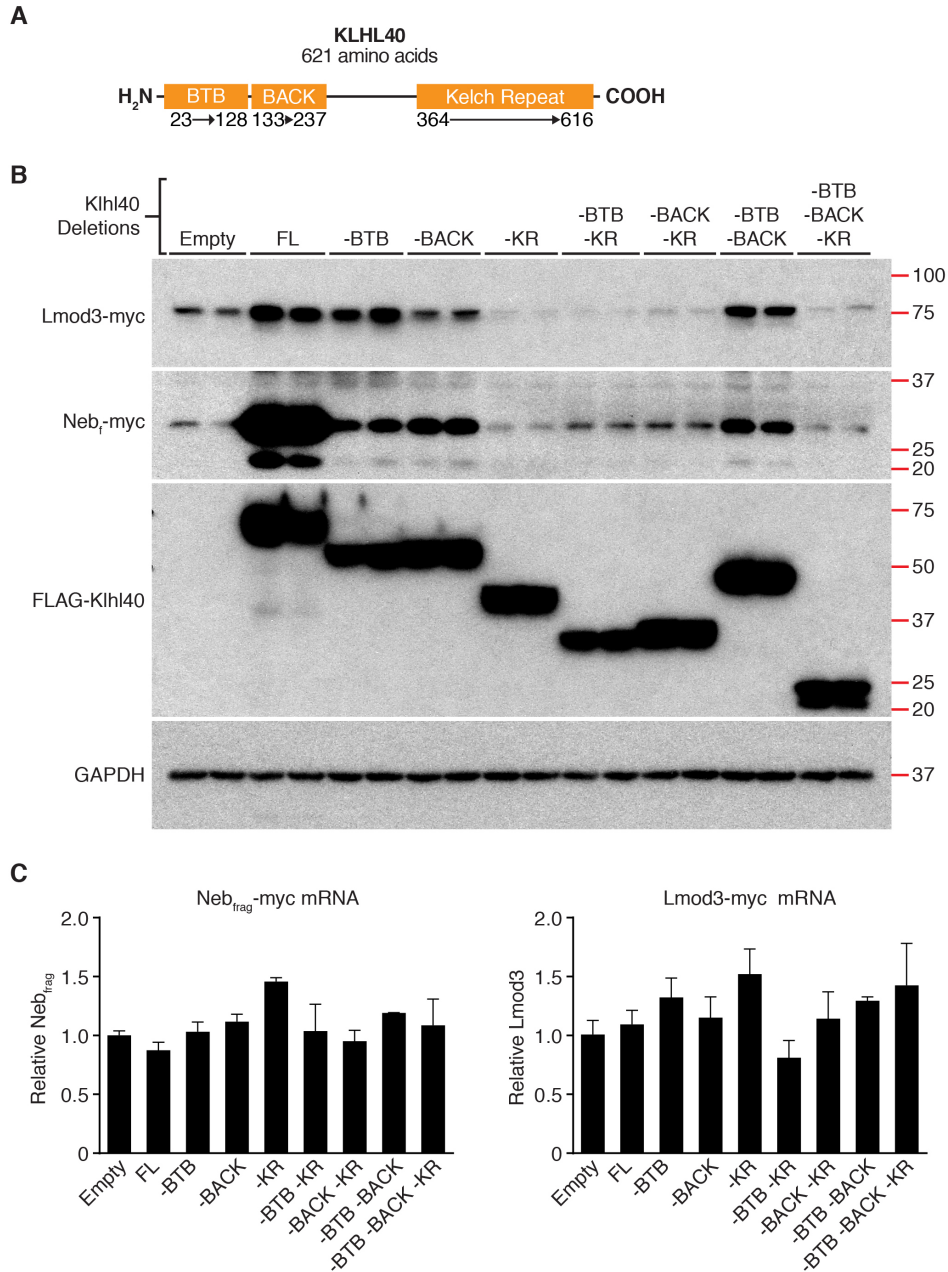
Supplemental Figure 10. Striated muscle specificity of *Lmod2* and *Lmod3*. qPCR analysis was performed using primers specific for *Lmod2* and *Lmod3* transcripts on the indicated adult mouse tissues. Signal only appears in striated muscle for both transcripts, but in a reciprocal manner. All values are normalized to 18S. SK muscle, skeletal muscle; WAT, white adipose tissue.



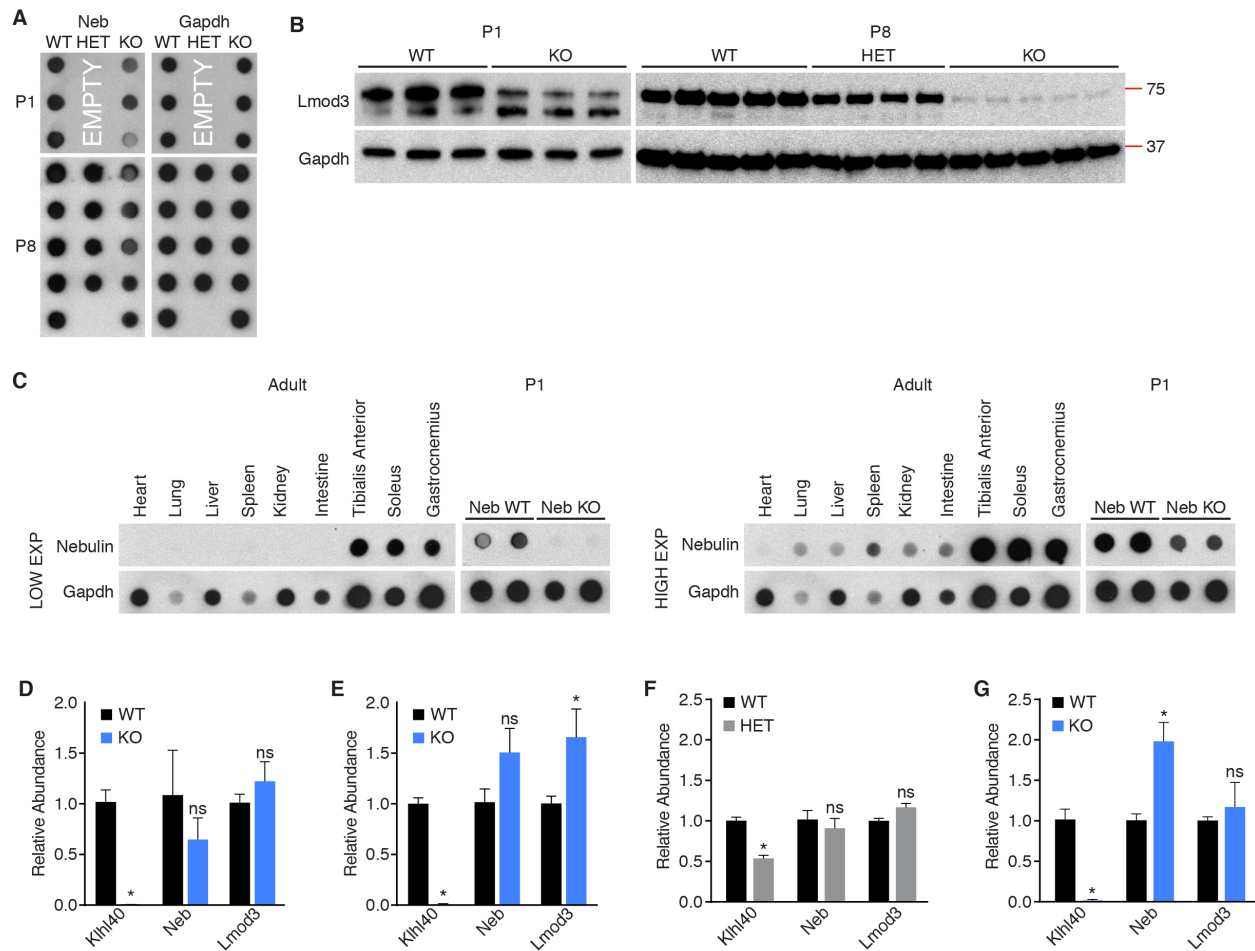
Supplemental Figure 11. *Neb_{frag}-myc* and *Lmod3-myc* mRNA expression in COS7 cells with or without FLAG-Kih140 co-expression in the absence and presence proteasome inhibitor. Corresponding qPCR analysis of *Neb_{frag}-myc* and *Lmod3-myc* expression of cells from Figure 5 and Supplemental Figure 12A shows that *Neb_{frag}* and *Lmod3-myc* expression does not change with the addition of Kih140. Expression of these transcripts is modestly increased upon introduction of proteasome inhibitor. All values are normalized to 18S and N=3 for all groups. * statistically significant difference with a false discovery rate (FDR) of 0.05. Data are presented as mean \pm SEM.



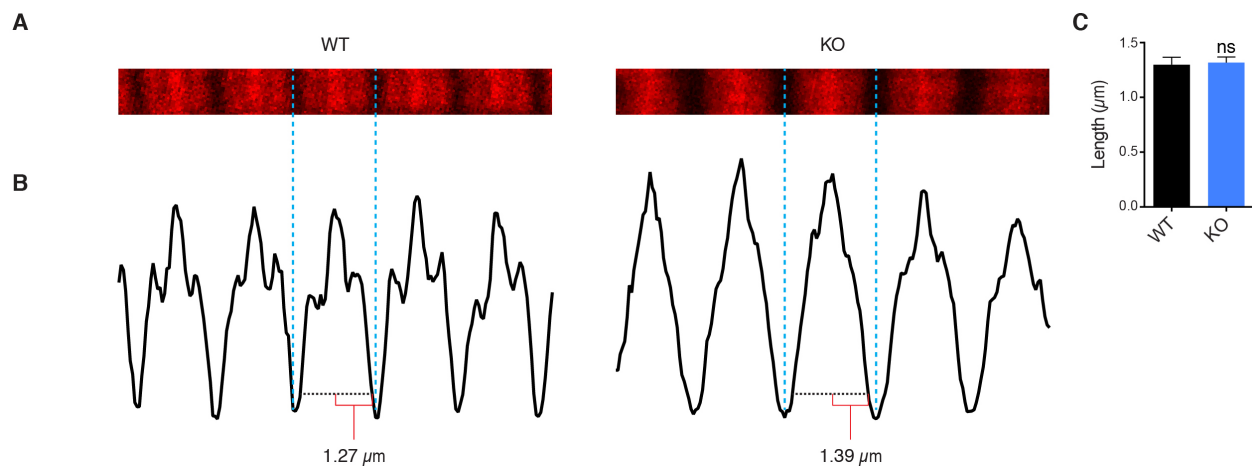
Supplemental Figure 12. Proteasome inhibition dramatically increases Lmod3 and Klh40 inhibits Lmod3 ubiquitination. (A) Klh40 regulation of Neb_{frag}-myc and Lmod3-myc in the absence or presence of 10 μ M MG132. Note that DMSO treated cells are data reproduced from Figure 5. Proteasome inhibition dramatically increases Lmod3-myc, but not Neb_{frag}-myc levels without dramatic changes in *Lmod3-myc* and *Neb_{frag}-myc* transcripts (Supplemental Figure 11). (B) Ubiquitination of Lmod3 protein in COS7 cells in the absence or presence of Klh40 shows decreased Lmod3-myc ubiquitination in the presence of Klh40. Ubiquitinated Lmod3-myc is denoted with a red bracket and a “Ub” label.



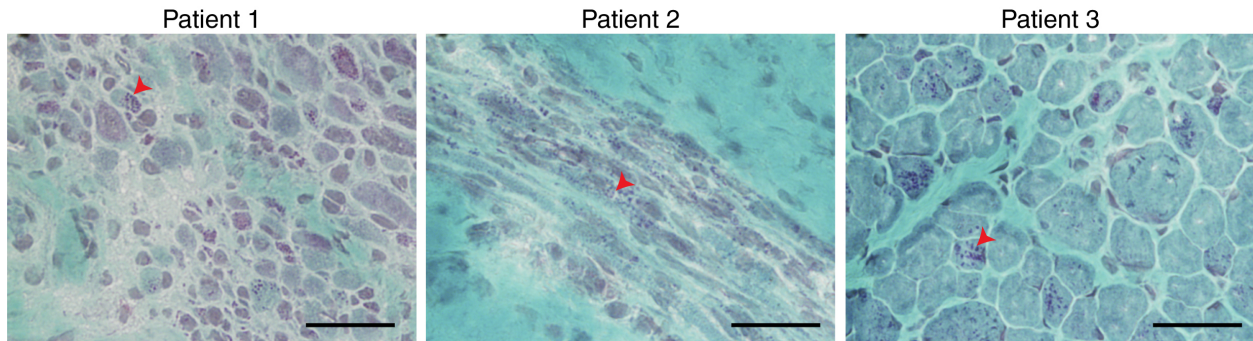
Supplemental Figure 13. Analysis of Khl40 domains required for Neb_{frag}-myc and Lmod3-myc stabilization. (A) Schematic representation of Khl40 protein. Numbers listed below domains indicate amino acid numbers that bound the respective domain. (B) Stabilization of Neb_{frag}-myc and Lmod3-myc in COS7 cells following co-expression with various domain deleted FLAG-Khl40 constructs. FL indicates full-length Khl40, while -BTB, -BACK, -KR, or any combination thereof indicate Khl40 lacking the specified domain(s). (C) Corresponding qPCR analysis of Neb_{frag}-myc and Lmod3-myc expression of cells shows that expression of these two transcripts does not change substantially between each of the indicated test groups. Co-transfection of the Khl40 mutant is indicated below each graph. All values are normalized to 18S and N=2 for all groups. Data are presented as mean ± SEM.



Supplemental Figure 14. Reduced Neb and Lmod3 in *Khl40* deficient mice without reduction of *Neb* and *Lmod3* mRNA. (A) Dot blot analysis of Neb and Gapdh (loading control) in P1 and P8 *Khl40* KO mice used to generate densitometry analysis in Figure 6A. Note that P1 samples only include WT and KO. (B) Western blot analysis of Lmod3 and Gapdh in P1 and P8 *Khl40* KO mice used to generate densitometry analysis in Figure 6B. Note that, for consistency, only the top band of P1 Lmod3 data is used for densitometry analysis since lower molecular weight bands did not appear in P8 samples. (C) Validation of Neb dot blot. Analysis of nebulin (Neb) signal in multiple adult tissues and skeletal muscle from P1 *Neb*^{+/+} and *Neb*^{-/-} mice [from (3)] shows that signal is specific to Neb in skeletal muscle. However, upon high exposure, some non-specific signal is apparent. Gapdh serves as a loading control. (D-G) qPCR analysis of *Khl40*, nebulin (*Neb*), and *Lmod3* in quadriceps of (D) P1, (E) and (F) P8, and (G) P6 *Khl40* WT, HET, and KO mice as indicated. *Khl40* is undetectable in KO mice and decreased by 50% in HET mice. *Neb* and *Lmod3* are not decreased for any genotype at any of the indicated ages. For (D) n=4, for (E), n=3, for (F) n=4, and for (G) n=3 for each indicated genotype in each panel. All values are normalized to 18S. * statistically significant difference with a false discovery rate (FDR) of 0.05. Data are presented as mean ± SEM.



Supplemental Figure 15. Sarcomere thin filament lengths are not decreased in Kihl40 KO mice. (A) Representative image of thin filament arrays labeled with phalloidin from stretched tibialis anterior muscles from P5 WT and KO mice. (B) Corresponding line scan analysis of previous thin filament arrays showing measurement of thin filament lengths. It is unknown why WT muscles had increased intensities near the pointed end of actin filaments. (C) Summary of thin filament length measurements show no difference between WT and KO muscles. N=32 sarcomeres for WT arrays and N=26 sarcomeres for KO arrays. Sarcomere measurements were done from 6 independent arrays (each from a different myofiber) combined from two separate mice for each genotype (3 arrays per mouse). Data are presented as mean \pm SEM.



Supplemental Figure 16. Muscle biopsies of KIH140 deficient patients. Gomori trichrome stain of skeletal muscle from Patient 1, Patient 2, and Patient 3. Sections for Patient 1 and Patient 3 show transverse fibers while the section for Patient 2 shows longitudinal fibers. Red arrowheads denote the presence of nemaline bodies which appear as punctate basophilic structures. Compared to Patient 3, Patient 1 and Patient 2 display increased collagen deposition and Patient 1 shows substantial fiber size heterogeneity. Scale bars: 25 μ m.

References Cited

1. Shelton, J.M., Lee, M.H., Richardson, J.A., and Patel, S.B. Microsomal triglyceride transfer protein expression during mouse development. *J Lipid Res.* 2000;41(4):532-537.
2. Millay, D.P., et al. Myomaker is a membrane activator of myoblast fusion and muscle formation. *Nature.* 2013;499(7458):301-305.
3. Bang, M.L., et al. Nebulin-deficient mice exhibit shorter thin filament lengths and reduced contractile function in skeletal muscle. *J Cell Biol.* 2006;173(6):905-916.
4. Ottenheijm, C.A., et al. Deleting exon 55 from the nebulin gene induces severe muscle weakness in a mouse model for nemaline myopathy. *Brain.* 2013;136(Pt 6):1718-1731.
5. Schindelin, J., et al. Fiji: an open-source platform for biological-image analysis. *Nat Methods.* 2012;9(7):676-682.
6. Kitamura, T., Onishi, M., Kinoshita, S., Shibuya, A., Miyajima, A., and Nolan, G.P. Efficient screening of retroviral cDNA expression libraries. *Proc Natl Acad Sci U S A.* 1995;92(20):9146-9150.
7. Wang, Z., Jiang, H., Chen, S., Du, F., and Wang, X. The mitochondrial phosphatase PGAM5 functions at the convergence point of multiple necrotic death pathways. *Cell.* 2012;148(1-2):228-243.
8. Horton, R.M. PCR-mediated recombination and mutagenesis. SOEing together tailor-made genes. *Mol Biotechnol.* 1995;3(2):93-99.
9. Ravenscroft, G., et al. Mutations in KLHL40 are a frequent cause of severe autosomal-recessive nemaline myopathy. *Am J Hum Genet.* 2013;93(1):6-18.
10. Littlefield, R., and Fowler, V.M. Measurement of thin filament lengths by distributed deconvolution analysis of fluorescence images. *Biophys J.* 2002;82(5):2548-2564.